Fisheries and Oceans Canada | Pêches et Océans Canada
Ecosystems and Oceans Science | Sciences des écosystèmes et des océans

Canadian Science Advisory Secretariat (CSAS)

Research Document 2015/071

Québec Region

Chemical and Biological Oceanographic Conditions in the Estuary and Gulf of St. Lawrence during 2014

L. Devine, S. Plourde, M. Starr, J.-F. St-Pierre, L. St-Amand,
P. Joly and P. S. Galbraith

Fisheries and Oceans Canada
Maurice Lamontagne Institute
850 de la Mer, P. O. Box 1000
Mont-Joli, QC, G5H 3Z4

December 2015

Canada

Foreword

This series documents the scientific basis for the evaluation of aquatic resources and ecosystems in Canada. As such, it addresses the issues of the day in the time frames required and the documents it contains are not intended as definitive statements on the subjects addressed but rather as progress reports on ongoing investigations.

Research documents are produced in the official language in which they are provided to the Secretariat.

Published by:

Fisheries and Oceans Canada
Canadian Science Advisory Secretariat
200 Kent Street
Ottawa ON K1A 0E6

http://www.dfo-mpo.gc.ca/csas-sccs/
csas-sccs@dfo-mpo.gc.ca

ISSN 1919-5044

Correct citation for this publication:

Devine, L., Plourde, S., Starr, M., St-Pierre, J.-F., St-Amand, L., Joly, P. and Galbraith, P. S. 2015. Chemical and Biological Oceanographic Conditions in the Estuary and Gulf of St. Lawrence during 2014. DFO Can. Sci. Advis. Sec. Res. Doc. 2015/071. v + 46 pp.

TABLE OF CONTENTS

ABSTRACT

An overview of chemical and biological oceanographic conditions in the Gulf of St. Lawrence (GSL) in 2014 is presented as part of the Atlantic Zone Monitoring Program (AZMP). AZMP data as well as data from regional monitoring programs are analyzed and presented in relation to long-term means in the context of a strong warming event that began in 2010 that was somewhat attenuated in 2014. Phytoplankton and zooplankton abundance indices and nutrient inventories were relatively coherent through the time series (1999–2014) between the high-frequency monitoring sites and among sections and subregions. Late-winter nutrient inventories were near or above normal in 2014, continuing the overall positive tendency that began in 2013. The spring bloom began later than had been observed in recent years, which coincided with the colder overall conditions in fall 2013/winter 2013–2014 (delayed ice retreat). In addition, the spring bloom magnitude was below normal and of shorter duration across the region. The differences between winter (maximum) and late spring (minimum) nitrate inventories were below normal in many regions of the GSL, confirming that primary production was lower than normal during spring 2014. In fall, chlorophyll *a* levels were nevertheless above normal in many regions of the GSL. For a third consecutive year, highly positive deep-water (> 200 m) nitrates were associated with high temperature and salinity. Conditions in the GSL were different compared to the St. Lawrence Estuary, where chlorophyll *a* was above normal during spring, summer, and fall. A striking increase in the relative abundance of diatoms was also seen at Rimouski station but not at Shediac Valley. The strong spring freshet affected the zooplankton community (lower abundances of *Calanus finmarchicus* and modified phenology), and overall higher temperatures and salinities likely resulted in increased abundances of warm-water copepod species. In contrast, water temperatures in the southern Gulf were near normal and phytoplankton abundance was high, both of which appeared to influence the zooplankton community in a coherent way. Our results and independent evidence from ecosystem surveys indicate that modifications to the abundance of large zooplankton might be due to a combination of environmental conditions (bottom-up processes) and an increase in predation pressure (top-down processes).

Les conditions océanographiques chimiques et biologiques dans l'estuaire et le golfe du Saint-Laurent en 2014

RÉSUMÉ

Un aperçu des conditions océanographiques chimiques et biologiques dans le golfe du Saint-Laurent (GSL) en 2014 est présenté dans le cadre du Programme de monitorage de la zone atlantique (PMZA). Les données du PMZA, ainsi que des données provenant de programmes de monitorage régionaux, sont analysées et présentées par rapport à des climatologies à long terme dans le contexte d'un événement de fort réchauffement qui a débuté en 2010 mais qui a été atténué en 2014. Les divers indices d'abondance du phytoplancton et zooplancton ainsi que les inventaires de sels nutritifs étaient relativement cohérents à travers les séries temporelles (1999–2014) entre les sites de surveillance à haute fréquence, les sections et les sous-régions. Les inventaires de sels nutritifs à la fin de l'hiver étaient près ou au-dessus de la normale en 2014, poursuivant la tendance positive globale initiée en 2013. La floraison printanière a été plus tardive que ce qui avait été observé au cours des dernières années. Ce changement coïncide avec les conditions globales plus froides de l'automne 2013 et hiver 2013–2014 (fondement tardif de la glace). En outre, l'ampleur de la floraison était inférieure à la normale et d'une plus courte durée sur toute la région. Les différences des stocks de nitrate entre l'hiver (maximum) et la fin du printemps (minimum) étaient inférieures à la normale dans de nombreuses régions de la GSL, confirmant que la production primaire était inférieure à la normale au cours du printemps 2014. En automne, le niveau de chlorophylle *a* a été néanmoins supérieur à la normale dans de nombreuses régions du GSL. Pour une troisième année consécutive, les anomalies de nitrate hautement positives en profondeur (> 200 m) ont été associées aux eaux avec de hautes valeurs de température et salinité. Les conditions dans le GSL étaient différentes par rapport à celles observées dans l'estuaire du Saint-Laurent, où la chlorophylle *a* été supérieure à la normale au cours du printemps, de l'été et l'automne. Une forte augmentation de l'abondance relative des diatomées a également été observée à la station de Rimouski, mais pas à la station vallée de Shediac. La forte crue printanière pourrait avoir influencé la communauté de zooplancton en engendrant des abondances de *Calanus finmarchicus* plus faibles ainsi qu'une phénologie modifiée. Les températures et les salinités globales plus élevées ont probablement aussi entraîné une augmentation des abondances des espèces de copépodes d'eau chaude. En revanche, les températures de l'eau dans le sud du golfe étaient près de la normale et l'abondance du phytoplancton était élevée; ces conditions semblaient influencer la communauté de zooplancton d'une manière cohérente. Nos résultats, ainsi que des observations indépendantes provenant du relevé écosystémique, suggèrent que les modifications dans l'abondance des grandes espèces de zooplancton pourraient être dues à une combinaison de conditions environnementales (processus «ascendants») et une augmentation de la pression de prédation (processus «descendants»).

INTRODUCTION

The Atlantic Zone Monitoring Program (AZMP) was implemented in 1998 (Therriault et al. 1998) with the aim of (1) increasing Fisheries and Oceans Canada's (DFO) capacity to understand, describe, and forecast the state of the marine ecosystem and (2) quantifying the changes in the ocean's physical, chemical, and biological properties and the predator–prey relationships of marine resources. A critical element in the observational program of AZMP is an annual assessment of the distribution and variability of nutrients and the plankton they support.

A description of the spatiotemporal distribution of nutrients (nitrate, silicate, phosphate) and oxygen dissolved in seawater provides important information on water-mass movements and on the locations, timing, and magnitude of biological production cycles. A description of phytoplankton and zooplankton distribution provides important information on the organisms forming the base of the marine food web. An understanding of plankton production cycles is an essential part of an ecosystem approach to fisheries management.

The AZMP derives its information on the state of the marine ecosystem from data collected at a network of sampling locations (high-frequency monitoring sites, cross-shelf sections) in each DFO region (Québec, Gulf, Maritimes, Newfoundland; see Fig. 1 for Québec region locations) sampled at a frequency of weekly to once annually. The sampling design provides basic information on the natural variability in physical, chemical, and biological properties of the Northwest Atlantic continental shelf: cross-shelf sections provide detailed geographic information but are limited in their seasonal coverage while critically placed high-frequency monitoring stations complement the geography-based sampling by providing more detailed information on temporal (seasonal) changes in ecosystem properties.

In this document, we review the chemical and biological oceanographic (lower trophic levels) conditions in the Gulf of St. Lawrence (GSL) in 2014. While indicators driven by winter air temperature (e.g., winter cold surface-layer volume, ice volume, summertime cold intermediate layer) showed cooler conditions overall in 2014 compared to the last few years (since 2010), indicators of summertime near-surface temperatures and deep-water (> 150 m) temperatures were at or near record highs (Galbraith et al. 2015). This report describes changes in the annual production cycles and community composition of phytoplankton and zooplankton in this context.

METHODS

All sample collection and processing steps meet and often exceed the standards of the AZMP protocol (Mitchell et al. 2002). All data included in this report were collected along seven sections during surveys done in June and October–November of each year and at two high-frequency monitoring sites (also called "fixed stations"; Fig. 1). Table 1 and Figure 2 show the 2014 surveys and the effort at high-frequency sampling sites, respectively. Rimouski station (RS) has been sampled since 1991 as part of a research project—about weekly throughout the summer, less frequently in early spring and late fall, and never in winter (except for physical variables during the March helicopter survey). It has been included in AZMP's annual review of environmental conditions since 2004 (AZMP 2006) to represent conditions in the St. Lawrence Estuary (SLE) and the northwest GSL. Since the beginning of the AZMP, Shediac Valley station (SV) has represented conditions in the southern GSL and SLE outflow.

Since 1996, a survey has been conducted of the winter surface mixed layer of the GSL in early to mid-March using a Canadian Coast Guard helicopter; surface nutrients (2 m) were added to the sampling protocol in 2001 (Galbraith 2006, Galbraith et al. 2006). This survey has added a considerable amount of data to the previously sparse winter sampling in the region. A total of 79

stations were sampled during the 3–18 March 2014 survey. The temperature and salinity of the 2014 mixed layer are described by Galbraith et al. (2015).

Near-surface phytoplankton biomass has been estimated from ocean colour data collected by the Sea-viewing Wide Field-of-view Sensor (SeaWiFS) satellite launched by NASA in late summer 1997 and by the Moderate Resolution Imaging Spectroradiometer (MODIS) "Aqua" sensor launched by NASA in July 2002. Here, MODIS data from January 2008 until December 2014 are combined with SeaWiFS data from September 1997 until December 2007 to construct composite time series of surface chlorophyll *a* (chl *a*) in four GSL subregions (northwest and northeast GSL, Magdalen Shallows, Cabot Strait; see Fig. 3 for locations). The performance of the MODIS satellite to estimate chl *a* has been compared with that of SeaWiFS for some regions of the globe. Although differences in sensor design, orbit, and sampling between MODIS and SeaWIFS cause some differences in calculated chl *a* values (Gregg and Rousseaux 2014), the performance of both satellites is relatively good and comparable. The biases associated with the different satellites are overall not significantly greater than algorithm uncertainties, particularly in non-turbid waters (Zibordi et al. 2006, Arun Kumar et al. 2015).

All selected subregions are located outside of the St. Lawrence River plume because data in regions influenced by this freshwater are unreliable due to turbidity and riverine input of terrestrially derived coloured matter. Composite satellite images were provided by BIO's remote sensing unit (Bedford Institute of Oceanography, DFO, Dartmouth, NS) in collaboration with NASA's GSFC (Goddard Space Flight Center). Basic statistics (mean, range, standard deviation) are extracted from two-week average composites with a 1.5 km spatial resolution.

We used the shifted Gaussian function of time model to describe characteristics of the spring phytoplankton bloom based on the combined satellite data (Zhai et al. 2011). Four different metrics were computed to describe the spring bloom characteristics: start date (day of year), cycle duration (days), magnitude (the integral of chl *a* concentration under the Gaussian curve), and amplitude (maximum chl *a*). In addition, we computed the mean chlorophyll biomass during spring (March to May), summer (June to August), and fall (September to December) as well as its annual average (March to December). For each of these eight metrics, we computed normalized annual anomalies (see below) to evaluate evidence of temporal trends among the different statistical subregions.

Chlorophyll *a* and nutrient data collected along the AZMP sections and at fixed stations were integrated over various depth intervals (i.e., 0–100 m for chl *a*; 0–50 m and 50–150 m for nutrients) using trapezoidal numerical integration. The surface (0 m) data were actually the shallowest sampled values; data at the lower depths were taken as either (i) the interpolated value when sampling was below the lower integration limit or (ii) the closest deep-water sampled value when sampling was shallower than the lower integration limit. Integrated nitrate values from the helicopter survey were calculated using surface concentrations (2 m) × 50 m; it was assumed that nitrate concentrations are homogeneous in the winter mixed layer at that time of the year.

In this document, we give a detailed description of the seasonal patterns in zooplankton indices for RS and SV. In recent years, the number and type of zooplankton indices as well as the way they are reported have been rationalized with the aim of standardizing research documents among AZMP regions. We thus present total zooplankton biomass, total copepod abundance, the relative contributions of the 10 most abundant copepod species, and *Calanus finmarchicus* and *Pseudocalanus* spp. (RS only) abundance and stage composition for the high-frequency monitoring sites. Because of its importance to the total zooplankton biomass in this region, a detailed description of *Calanus hyperboreus* was added. We present the spring and fall total zooplankton biomass and total abundance of *C. finmarchicus*, *C. hyperboreus,* and

Pseudocalanus spp. for three regions having distinct oceanographic regimes (Fig. 1) and corresponding more to the spatial scales addressed by AZMP in other regions:

(1) western GSL (wGSL): this region is generally deep (> 200 m) and cold in summer. It is strongly influenced by freshwater runoff from the St. Lawrence River and cold and dense waters from the Laurentian Channel;

(2) southern GSL (sGSL): this region is shallow (< 100 m) and much warmer in summer. It is under the influence of the Gaspé Current;

(3) eastern GSL (eGSL): this region, with deep channels and a relatively wide shelf (< 100 m), is characterized by higher surface salinity and is directly influenced by the intrusion of water from the Labrador and Newfoundland shelves.

Standardized anomalies of key chemical and biological indices were computed for the high-frequency sampling stations, sections, and oceanographic regions. These anomalies are calculated as the difference between the variable's average for the season (i.e., chlorophyll and nutrient indices) or for the complete year (i.e., zooplankton indices) and the variable's average for the reference period (usually 1999–2010); this number is then divided by the reference period's standard deviation. Only actual measurements were used for these calculations, not modelled data. These anomalies thus represent observations in a compact format. A standard set of indices representing anomalies of nutrient availability, phytoplankton biomass and bloom dynamics, and the abundance of dominant copepod species and groups (*C. finmarchicus, Pseudocalanus* spp., total copepods, and total non-copepods) are produced for each AZMP region (see DFO 2015). We also present several zooplankton indices that reflect either different functional groups with different roles in the ecosystem or groups of species indicative of cold- or warm-water intrusions and/or local temperature conditions: large calanoids (dominated by *Calanus* and *Metridia* species), small calanoids (dominated by more neritic species such as *Pseudocalanus* spp., *Acartia* spp., *Temora longicornis*, and *Centropages* spp.), cyclopoids (dominated by *Oithona* spp. and *Triconia* spp.; the latter is a poecilostomatoid that is included in this category because of its ecological characteristics), warm-water species (*Metridia lucens, Centropages* spp., *Paracalanus* spp., and *Clausocalanus* spp.), and cold/arctic species (*Calanus glacialis* and *Metridia longa*).

Potential changes in zooplankton phenology were explored using *C. finmarchicus* as an indicator. We used the time series at RS because adequate sampling and stage identification started there 20 years ago (1994). From 1994 to 2004, *C. finmarchicus* copepodite stage abundance was determined using samples collected with 333 µm (CIV–CVI) and 73 µm (CI–III) mesh nets that were analyzed for seven years of the time series (see Plourde et al. 2009 for details). In other years before 2004 for which 73 µm samples were not analyzed, the abundance of CI–III in the 333 µm samples was adjusted based on a comparison done with an AZMP-like net (S. Plourde, DFO, unpublished data). The phenology of *C. finmarchicus* was described using the normalized (x/x_{max}) relative stage proportions within each year for CI–III, CIV, CV, and CVI (male and female). This method differs from the one used in previous reports (2013 and earlier), where normalization was calculated over the whole period (1994–2013). Prior to the calculation of proportion, stage abundance data (ind m^{-2}) were smoothed using the Loess algorithm.

RESULTS

NUTRIENTS AND PHYTOPLANKTON

Distributions of the primary dissolved inorganic nutrients (nitrate, silicate, phosphate) included in AZMP's observational program strongly co-vary in space and time (Brickman and Petrie 2003). For this reason and because the availability of nitrogen is most often associated with phytoplankton growth limitation in coastal waters of the GSL, emphasis in this document is placed on variability in nitrate concentrations and inventories.

High-frequency monitoring sites

The Rimouski and Shediac Valley stations typically exhibit a biologically mediated reduction in surface nitrate inventories in spring/summer, a minimum during summer, and a subsequent increase during fall/winter (Fig. 4), although the 2014 fall sampling at SV ended before this increase was observed. The nutrient draw-down occurs later at RS compared to SV, reflecting the later spring bloom in the St. Lawrence Estuary (May–July in 2014) compared to SV (April). In contrast to SV, surface (0–50 m) nutrient inventories at RS remain relatively high during summer and usually at levels non-limiting for phytoplankton growth. These high levels are mainly the result of upwelling at the head of the Laurentian Channel and the high tidal mixing in this area, and to some degree to anthropogenic and river sources, notably from the St. Lawrence River.

In 2014, nutrient levels at RS followed the long-term pattern fairly closely despite the higher-than-normal chlorophyll levels throughout the season (Fig. 4).The early spring bloom at SV was not captured by the 2014 sampling. Nevertheless, evidence of a bloom is seen in the drop in nitrate levels between the March helicopter survey and the first ship-based sampling in April (Fig. 4). Nitrate and chl *a* levels at that station were generally close to the 1999–2010 mean, although chl *a* was somewhat lower from May through July.

At RS, total phytoplankton abundance was near normal, but diatom abundance was above the long-term mean and ciliates below for the first time since 2011; flagellates and especially dinoflagellates continued to show negative anomalies (Fig. 5). The phytoplankton community had been regularly dominated by diatoms throughout the sampling period between 1999 and 2003, and a shift from diatoms towards flagellates and dinoflagellates was observed between 2004 and 2013 (Fig. 5). This situation changed strikingly in 2014, with positive anomalies in the diatom/dinoflagellate and diatom/flagellate ratios for the first time since 2004. The seasonal pattern of the major phytoplankton groups was very different from the reference period due to a sharp increase in the relative contribution of diatoms in fall (and dinoflagellates from October), with the concomitant near-disappearance of flagellates, which usually dominate at this time (Fig. 6).

The situation was very different at SV compared to RS in 2014: diatom abundances were lower compared to the long-term average while flagellates and ciliates both showed strong positive anomalies (Fig. 7). The abbreviated sampling period (only four samples were analyzed: 21 May, 11 July, 13 Aug., 15 Sept.) does not allow much comment to be made concerning the seasonal evolution of the phytoplankton community composition, but greater proportions of flagellates and especially ciliates were observed in July–August, a period when diatoms generally dominate the community (1999–2010 reference period) (Fig. 6).

Sections and late winter helicopter survey

Late winter nitrate concentrations in 2014 were relatively high at the surface for most regions of the GSL (Fig. 8). The highest winter surface nitrate concentrations were observed off the Gaspé Peninsula, and concentrations gradually decreased from west to east. No sampling was done in

the SLE because of logistic constraints (lack of ice to land on), but transport of nutrient-rich water from the Estuary towards the southern GSL was clearly evident. The winter maximum nutrient inventories in 2014 showed the first wide-spread positive anomalies since 2007 (compared to the 2001–2010 average; Fig. 9, 10), thus definitively ending the period of strong negative anomalies that was evident in 2010–2011 and to a lesser extent in 2012. This is consistent with the fact that winter mixing was higher than normal in 2014 (Galbraith et al. 2015).

Late spring surface nitrate inventories are always low compared to late winter inventories along the seven sections crossing the Estuary and GSL due to utilization by phytoplankton (Fig. 11). Spring nitrate levels in 2014 were slightly higher than those measured during the late fall survey for most areas. This indicates that the autumnal turnover had not yet occurred.

The late spring nitrate inventories in 2014 were generally well above the 1999–2010 reference period averages, similar to what was observed in 2013 (Fig. 10). This suggests that spring primary production may have been lower than usual. While this is not readily apparent when examining the time series of chlorophyll levels measured during field sampling (Fig. 12) and spring chlorophyll anomalies are neutral on the scorecard (Fig. 10), we see some evidence for this in the MODIS imagery (Fig. 13b; largely negative anomalies over much of the Gulf).

The differences between the winter maximum nitrate inventories and the late spring minimum inventories along the sections were mostly below average, a trend that has been apparent since 2008 (Fig. 10). This index represents the pool of nutrients that was potentially used by phytoplankton during spring. A negative index indicates lower new phytoplankton production with potential detrimental effects on higher trophic levels. The 2014 fall surface nitrate inventories were also mostly near or below the 1999–2010 mean. Examination of the standardized scorecard anomalies shows a variable pattern in the seasonally adjusted nitrate inventory (0–50 m), with positive anomalies in the western/central Gulf (TASO and TCEN transects), a negative anomaly at Cabot Strait (TDC), and neutral values elsewhere. Nearly all deep-water nitrate inventories showed strongly positive anomalies, as they have since 2012, with the exception of the Estuary transect (TESL). Fall chlorophyll anomalies were overall above the long-term mean, while the spring levels were overall close to the normal (Fig. 10). The patterns seen for the Estuary transect (sampled twice in 2014) agree well with those from RS, which was sampled weekly from May through October (Fig. 4, 10).

Remote sensing of ocean colour

Satellite ocean colour data provide large-scale images of surface phytoplankton biomass (chl *a*) over the whole NW Atlantic. We used two-week satellite composite images of four GSL subregions to supplement our ship-based observations and provide seasonal coverage and a large-scale context over which to interpret our survey data. The ocean colour imagery provides information about the timing and spatial extent of the spring and fall blooms but does not provide information on the dynamics that take place below the top few metres of the water column. In addition, satellite ocean colour data for the St. Lawrence Estuary are largely contaminated by high concentrations of nonchlorophyllous matter originating from the continent (such as suspended particulates and coloured dissolved organic matter) that render these data too uncertain to be used. Knowledge of phytoplankton dynamics in the St. Lawrence Estuary and the subsurface information are gathered using the high-frequency sampling at Rimouski station and the broad-scale oceanographic surveys.

Satellite images in 2014 revealed considerable spatial variability in the timing of the spring bloom in the GSL (Fig. 13), as has been previously observed (not shown), likely due to subregional differences in the timing of sea-ice melt and the onset of water column stratification (Le Fouest et al. 2005). The spring phytoplankton bloom occurred between late April and early

June, depending on the region, and started earlier in the northwest and southern parts of the GSL (Fig. 13, 14). Satellite images from the same periods as the spring and fall mission (1–15 June and November; Fig. 14) do not shed much light on the interpretation of the chlorophyll anomalies calculated from samples taken during the missions. The composite image from early June shows some strong but patchy negative (in the eastern Gulf) and positive (in the western Gulf) anomalies whereas the anomalies from ship-based sampling are largely neutral (Fig. 10, 14). The same is true for the fall sampling, although no imagery data were available for large sectors of the Gulf. Furthermore, the composite satellite image from late October (Fig. 15) shows strong positive anomalies in the western and southern Gulf. The field samples from RS and SV only partly support these findings: while a strong peak is apparent for RS, SV is slightly below the 1999–2010 average (Fig. 4). These apparent mismatches between satellite imagery and ship-board sampling could be due to limitations inherent in both of the methods: we have already discussed those for the imagery data, and field samples represent point values (spatially and temporally) that might not be representative of patchy events.

The time series of surface chlorophyll concentrations calculated from satellite images show that fall blooms in the GSL are generally lower in magnitude than spring blooms (Fig. 16). In 2014, the onset of the spring bloom as revealed by satellite images was delayed in the four subregions even though peak values were above average. The most marked differences compared to the 1999–2010 averages were observed in the Magdalen Shallows and NWGSL. The Magdalen Shallows showed a peak value in July that was nearly as high as that in late April, and chlorophyll values increased again in September–October. A similar and even more striking pattern is seen in the NWGSL, where chlorophyll values increased throughout the summer to a secondary peak rivaling that of early May (Fig. 16).

The standardized scorecard anomalies inferred from the satellite imagery mirrored these observations (Fig. 17), with overall positive anomalies for the start of the spring bloom (i.e., a delay) and bloom amplitudes (i.e., peak chl *a* values) and negative anomalies in spring bloom durations and magnitudes. We also see the strong positive anomalies for surface chlorophyll in the Magdalen Shallows (June–August) and NWGSL (September–December). Since 1998, there has been a tendency toward gradual but significant increases in near-surface chlorophyll concentrations in the NWGSL and Magdalen Shallows areas that are driven by these late-summer/fall values.

ZOOPLANKTON

High-frequency monitoring sites

Figure 18 shows the long-term (RS: 2005–2010; SV: 1999–2010) seasonal climatologies of zooplankton biomass at the high-frequency monitoring stations along with observations made in 2014. The zooplankton biomass at RS in 2014 was generally above average throughout the season, with only a few points below the average in June (Fig. 18a); observations were well above the average throughout late summer and fall. At SV, zooplankton biomass was near normal all season with the exception of one high value in July and a low value in August (Fig. 18b). Results at this site must be considered carefully due to the low sampling frequency.

Total copepod abundance at RS in 2014 was near or above the average from April to June and increasingly higher than average throughout the rest of the sampling season (Fig. 19a). This higher-than-normal abundance of copepods corresponded to a higher-than-normal proportion of *Microcalanus* spp. in mid-summer and *Oithona similis* in late-summer/fall with concomitant decreases in the contributions of *Calanus finmarchicus* and *C. hyperboreus* among the 10 most abundant copepod species (Fig. 19b, c). Another notable feature observed in the deep samples of RS in 2014 was the replacement of *Paraeuchaeta norvegica* by species in the family

Aetideidae among the 10 most abundant taxa (Fig. 19b, c). At SV, the observed total copepod abundance in 2014 showed more extreme highs and lows than the average observations (Fig. 19d). The relative abundances of the dominant copepod species in 2014 showed some striking changes from the 1999–2010 average, with a marked increase in the *Temora longicornis* contribution in late summer, the delayed increase in *O. similis* (starting in July), and the low mid-summer contribution of *C. finmarchicus* (Fig. 19e, f).

As was observed in 2013, *C. finmarchicus* abundance at RS was well below normal except for a few samples scattered throughout the season (Fig. 20a), but the overall pattern of increase starting in late summer was still observed. The peak contribution of early stages—which had been shifted to August in 2013—was centred on July in 2014; this is still later than the June peak seen in the 2005–2010 time series (Fig 20b, c). The 2014 peak in early stages coincided with the period of very low population abundance whereas the higher abundances later in the season were mostly associated with stage CV. The abundance and pattern of copepodite stages at SV was very similar in 2013 and 2014, with lower-than-normal abundances early in the season returning to near normal by September; there was once again a peak in early stages (CI–III) centred on August (Fig. 20d, f). This pattern must be interpreted with caution since there was generally only one observation per month at this station in 2014.

The abundance of the large-bodied *C. hyperboreus* at RS in 2014 was near the long-term average early in the season and above average in fall (Fig. 21a) while abundances at SV were generally near normal throughout the season (Fig. 21d). Interestingly, a strong peak occurred at both stations in May. The relative abundances of the copepodite stages were very similar to the long-term patterns at both stations (Fig. 21b, c, e, f).

The abundance of *Pseudocalanus* spp. at RS was mostly above normal in 2014, especially from June until the end of the sampling period (Fig. 22a). The population stage composition averaged from 2005 to 2010 showed that early stages have been observed throughout the year (potential for several generations) (Fig. 22b), but the early copepodite stages were relatively more abundant in May 2014 than what is observed in the 2005–2010 average (Fig. 22c). *Pseudocalanus* spp. abundance at SV increased strikingly from May through July 2014 (markedly above the 1999–2010 average) and then decreased to below-normal values in August and for the rest of the sampling season (Fig. 22d). No stage analysis was carried out for this species at Shediac Valley.

Gulf subregions

The averaged total zooplankton biomass values for the GSL subregions during the spring and fall 2014 surveys were within the range of values seen throughout the time series, although the fall averages have tended to increase while the spring values have tended to decrease over the past few years (Fig. 23). In general, the total zooplankton biomass in the sGSL in spring shows greater interannual variability than in the other GSL regions and has been much higher than in fall for some years, although this difference has attenuated in 2013 and 2014. These marked differences in zooplankton biomass among years in the sGSL during the early part of the productive season have been previously ascribed to interannual differences in the influx of large-bodied *Calanus* spp. from deeper adjacent regions (Plourde et al. 2014). However, this pattern could also be caused by interannual variations in the spatial distribution of zooplankton biomass in the sGSL in June (de Lafontaine 1994), implying that samples taken on the TIDM section would not be always representative of the overall zooplankton population among years in this region.

Overall, the 2014 annual abundances of key copepod species in the three regions are consistent with patterns observed over the times series, and values have changed little since 2013 (Fig. 24, 25, 26). Some of these indices appear to be quite stable in different parts of the

study area (e.g., *C. finmarchicus* in the wGSL since 2008, *C. hyperboreus* in the wGSL and sGSL [fall only], *Pseudocalanus* spp. in the wGSL) while others vary greatly on different time scales, particularly in spring (e.g., *C. finmarchicus* and *C. hyperboreus* in sGSL, *Pseudocalanus* spp. in eGSL and sGSL). These variations in spring abundance of these key copepod species could be caused by interannual variations in overall population productivity, in the relative timing of the spring surveys and population development (phenology), or both. During fall surveys, interannual variations in *C. finmarchicus* and *C. hyperboreus* population abundance were mainly caused by fluctuations in the abundances of overwintering stages.

Copepod phenology

We present a detailed figure showing the seasonal cycle of the relative proportions of *C. finmarchicus* copepodite stages at Rimouski station from 1994 to 2014 in order to provide an assessment of potential changes in zooplankton phenology in the GSL (Fig. 27). The comprehensive examination of this data set revealed notable changes in the developmental timing of this key copepod species over the time series. For example, the period of maximum contribution of stages CI–III (equivalent to their abundance maximum) had gradually shifted from mid- to late July until mid-June from 1994–2012 and made a sudden shift back to late summer in 2013–2014 (Fig. 27). Relative CIV abundance showed a similar shift, and its maximum abundance is nearly concurrent with that of the CI–III stages. The trend toward earlier development in summer stages was also observed in CV until 2012, and this stage also showed evidence of later-summer increases in 2013–2014. The long-term change in the timing of maximum occurrence that we observed for stage CVI (both sexes)—with an earlier timing from 2008–2012 relative to 1994–2005—has shown some indication of shifting to later in the season in 2013–2014, although this is not so striking as it is for the early stages. The late occurrence of early stage (CI–CIII) abundance in the region in 2014 could result from an abnormally high freshet from the St. Lawrence River in May and June 2014 (Galbraith et al. 2015), and also from a later timing of the spring bloom (Fig. 17) due to a later ice break-up generally observed in many regions of the GSL including in the wGSL, a region highly connected with the Estuary in late summer and fall and contributing to the zooplankton in the Estuary (and RS) (Maps et al. 2011, Galbraith et al. 2015).

Scorecards

A synthesis of basic AZMP zooplankton indices (abundances of *C. finmarchicus*, *Pseudocalanus* spp., total copepods, non-copepods) was performed using annual standardized abundance anomalies and is presented as a scorecard (Fig. 28). The reference period used to standardize annual abundances with the whole time series ranges from 1999 (2005 for RS) to 2010. In general, these annual indices were relatively coherent through the time series at RS, SV, and within the large subregions. *C. finmarchicus* anomalies have remained overall negative since 2009 while the smaller *Pseudocalanus* spp. has shown a trend toward positive abundance anomalies since 2009, with especially strong positive anomalies in the western regions (RS, SV, wGSL). Total copepod abundance anomalies had been negative in 2012 and 2013 but returned to normal (sGSL, eGSL) or positive (RS, SV, wGSL) in 2014. Finally, the strong positive anomalies in non-copepod abundance that have been building in different regions since 2010 were positive in all regions in 2014, especially so at RS. The striking anomaly (~ 20 SD) observed for non-copepods at RS was mostly caused by high abundances of larvaceans (*Fritillaria* spp.), gastropods (*Limacina* spp.), cnidarians (*Aglantha digitale*), and polychaete larvae. This extreme anomaly can be explained by the very low variability and low abundance throughout most of the time series followed by a sudden sharp increase in the abundance of this group in 2014.

The annual standardized abundance anomalies for a set of zooplankton indices are presented in Figure 29. Again, these annual indices were relatively coherent among the fixed stations and large regions over the time series. The abundances of *C. hyperboreus*, small calanoids, cyclopoids, and warm-water copepods all showed tendencies toward more positive anomalies, especially the latter group, while large calanoids and cold-water copepods had normal or slightly negative anomalies (Fig. 29). Lower-than-normal abundances of large calanoids have been the norm in the GSL since 2009 (except for in 2012), which was particularly the case in the eGSL and sGSL in 2014. Small calanoid abundances increased to above-normal values in 2014 relative to 2013 (Fig. 29), which was due to strong positive *Pseudocalanus* spp. anomalies characteristic of the whole GSL (Fig. 28), and *Microcalanus* spp. at the deep RS (Fig. 19c). There were two striking results revealed by the 2014 scorecard. One was the strong positive anomalies for warm-water species in all regions except in the sGSL (Fig. 29). The other was the abundance of cold/arctic copepod species (*C. glacialis*, *M. longa*), which was below normal in several areas in 2013, showing near or slightly above normal anomalies over the whole GSL in 2014 (Fig. 29). Note that indices of warm-water and cold/arctic species are based on generally rare taxa, implying that relatively minor changes in abundance could result in large variations in their anomalies.

DISCUSSION

In 2014, physical indices driven by winter air temperature (e.g., winter surface layer, sea-ice, and summertime cold intermediate layer volumes) showed cooler conditions than those of the last few years while summertime surface and deep-water (> 150 m) temperatures were at or near record highs (Galbraith et al. 2015). This document reports on the chemical and biological conditions in the GSL in the context of these conditions.

Winter maximum surface nutrient inventories in 2014 were close to or above the 2001–2010 average throughout the GSL after a period of strong negative anomalies that was evident in 2010–2012. Winter mixing is a critical process to bring nutrient-rich deep water to the surface. In the GSL, this winter convection is in part caused by buoyancy loss (cooling and reduced runoff), brine rejection associated with sea-ice formation, and wind-driven mixing prior to ice formation (Galbraith 2006). Thus physical conditions in the Gulf led to a higher supply of start-up nutrients for primary producers in 2014 compared to the 2010–2012 period. In addition to vertical mixing, the upwelling at the head of Laurentian Channel and the transport of nutrients via the Gaspé Current may also have contributed to enhancing winter nutrient inventories for the estuarine portion and freshwater-influenced subregions of the GSL. Finally, water intrusions into Cabot Strait from south of Newfoundland were near normal in 2014 (Galbraith et al. 2015). Typically, these waters, which enter the Gulf via Cabot Strait during winter and flow in part northward along the west coast of Newfoundland, are relatively poor in nutrients compared to those that have originated from the Estuary or were mixed from deeper waters within the Gulf. However, high positive deep-water (> 200 m) nutrient anomalies have been observed since 2012 in all areas but the Estuary region, associated with high temperature and salinity intrusions into the Gulf from Cabot Strait (Galbraith et al. 2015).

In contrast to expectations based on winter nutrient inventories, ocean colour data as well as the spring nitrate inventories revealed that the magnitude of the spring phytoplankton bloom in 2014 was below normal and of shorter duration across the region. In addition, phytoplankton growth was initiated later than in recent years in many regions. Changes in ice cover can influence primary production by its influence on the light conditions in the water column (Le Fouest et al. 2005), and changes in stratification can also have either positive or negative effects on primary production depending on water column conditions (Ferland et al. 2011). The later-than-normal ice retreat and later warming/stratification (Galbraith et al. 2015) contributed to

the markedly late spring bloom in 2014 compared to recent years. The fact that utilization of nutrients during the spring was overall below normal in 2014 is consistent with this interpretation. In late summer and fall, chlorophyll *a* levels were nevertheless above normal in many regions of the GSL, coinciding with the warming of surface waters (Galbraith et al. 2015).

In the lower St. Lawrence Estuary, the situation is somewhat different: the timing of the bloom was near normal in 2014, but chlorophyll *a* was above normal from spring to late fall (measured at Rimouski station). Spring bloom timing in this region is recognized to be largely influenced by both runoff intensity and freshwater-associated turbidity (Levasseur et al. 1984, Therriault and Levasseur 1985; Zakardjian et al. 2000, Le Fouest et al. 2010, Mei et al. 2010). While the spring bloom typically starts just after the spring–summer runoff peak, this was not the case in 2014. Even though the annual average runoff of the St. Lawrence River in 2014 was near normal, the spring freshet was above normal and persisted much longer than usual, with higher-than-normal runoff in May and June (Galbraith et al. 2015). In this context, the unexpected above-normal phytoplankton biomass from May onward suggests that the phytoplankton growth rate largely compensated for losses due to physical transport (advection) and biological factors such as grazing by zooplankton, which could have be lower than usual in 2014 (see below). The above-normal runoff could also have promoted the transport of nutrients toward the northwestern and southern part of the Gulf, an area where unusually high chlorophyll concentrations were observed during summer (July–August 2014; Fig. 16).

The shift to a smaller-sized phytoplankton community observed in recent years at Rimouski station reversed in 2014, with positive anomalies in the diatom/flagellate ratio for the first time since 2004. This was largely the result of a sharp increase in the relative contribution of diatoms in fall with the concomitant near-disappearance of flagellates, which usually dominate at this time. This shift is consistent with the above-normal phytoplankton biomass and nutrient inventory in the region during fall. Diatoms are usually largely responsible for major changes in chlorophyll biomass and are associated with a nutrient-rich, well-mixed environment. In contrast, flagellates and dinoflagellates are associated with a nutrient-poor, stratified environment. In this context, it is interesting to note that the situation at SV in 2014 was very different compared to RS: diatom abundances were lower compared to the long-term average while flagellates showed strong positive anomalies. Warmer temperatures and stronger stratification, as observed in summer 2014 in the GSL but less so in the SLE (RS) (Galbraith et al. 2015), are associated with a shift toward greater flagellate and dinoflagellate predominance (Levasseur et al. 1984, Li and Harrison 2008), with potential consequences on copepod recruitment and zooplankton composition as well as on the flow of energy in marine food webs.

In 2014, deep-water temperatures and salinities were reported to be overall well above normal in the Gulf because of inward advection from Cabot Strait, where temperature and salinity reached record highs in 2012 at 200 and 300 m (Galbraith et al. 2015). The above-normal deep (300 m) nutrient levels that we observed are associated with this water mass. These elevated values of temperature, salinity, and nutrients indicate that a higher proportion of slope water was entering the GSL compared to Labrador Shelf water. Further investigation is clearly needed on this phenomenon, since it appears to be a recurrent event over the last few years (Galbraith et al. 2015). The warming of bottom waters and their above-normal nutrient levels (which will eventually be upwelled at the head of the Laurentian Channel) may have impacts on acidification previously reported in the region (Mucci et al. 2011), with potential negative consequences on fisheries and aquaculture activities as well as on overall productivity and biodiversity in the GSL.

Similar to what was observed in 2013, the higher-than-normal St. Lawrence freshwater runoff observed in May and June 2014 likely impacted the zooplankton community in the St. Lawrence Estuary. The most discernible consequences were the lower-than-normal abundance of *C.*

finmarchicus in summer, a later-than-normal timing of recruitment of early *C. finmarchicus* stages, and a contribution of CI–III to the population abundance of *C. hyperboreus* that was shorter than normal (restricted to May). However, the phytoplankton biomass observed at RS and in the wGSL in 2014 was greater than in 2013 and well above normal, which might have stimulated higher local zooplankton production, as suggested by the above-normal *C. finmarchicus* and *C. hyperboreus* abundances in late summer and fall and the strongly positive *Pseudocalanus* spp. abundance anomalies at RS. Therefore, this greater primary production in the wGSL seemingly has resulted in annual abundance anomalies of *C. finmarchicus* and *C. hyperboreus* near or above normal, respectively, both slightly greater than in 2013.

In 2013, deep-water temperatures and salinity averaged over the Gulf increased slightly to reach the highest value since 1980 (Galbraith et al. 2014). This warm anomaly was first observed in Cabot Strait a few years ago and has propagated northwestward into the Gulf to arrive at RS in 2014 (Galbraith et al. 2015). Combined with surface water temperatures that were well above normal in the eGSL and wGSL in summer, these conditions likely resulted in the well-above-normal (RS, wGSL, eGSL) abundances of warm-water copepod species in 2014. High positive anomalies in warm-water copepod species in the wGSL and at RS in 2013 were mostly caused by the high abundance of *M. lucens*, a mid-water species that might benefit from a warmer and saltier deep layer as well as from warmer conditions at the surface and in the CIL (cold intermediate layer). While *M. lucens* was still generally more abundant than normal in the wGSL, sGSL, and eGSL in 2014, the high positive anomalies in warm-water copepod species in 2014 in the eGSL and wGSL were also due to higher abundances of surface-dwelling and neritic *Paracalanus* spp. and *Centropages* spp., respectively. These two taxa showed strong interannual variability likely related to high-frequency variations in upper-ocean environmental conditions, whereas the deep-water *M. lucens* exhibited high anomalies over the last 4–5 years, likely associated with lower-frequency variations of the more stable deep-water characteristics (Galbraith et al. 2015). The arrival of these warmer-than-normal deep waters at RS in 2014 might also explain the increase in abundance of Aetideidae, a family composed of various deep-dwelling copepod species generally associated with deep oceanic regions.

Unlike the warm conditions observed throughout most of the Gulf, surface and water column temperatures in 2014 in the sGSL were near normal (see Fig. 17, 43–47 in Galbraith et al. 2015). In addition, phytoplankton biomass was generally greater-than-normal in summer and fall. This surface temperature regime and high phytoplankton biomass probably had a strong impact on the zooplankton community in the region: contrary to the rest of the GSL, abundance anomalies of warm-water and cold-water copepod species were near or above normal in the sGSL, consistent with the region being cooler than the wGSL and eGSL. The higher-than-normal proportion of *T. longicornis* and strong positive anomalies of *Pseudocalanus* at SV and in the sGSL in 2014 could represent a response to higher-than-normal phytoplankton biomass in the region in summer and fall. Finally, the cooler summer conditions at SV and in the sGSL might be the consequence of a reduced influence from the upstream wGSL, as suggested by currents (0–20 m, 20–100 m) predominantly concentrated along the northern margin of the sGSL in spring 2014 (Galbraith et al. 2015). It has been hypothesized that a high spring freshwater runoff from the St. Lawrence River, which was the case in 2014, could result in a lower transport of *Calanus* species in the sGSL (Runge et al. 1999, Galbraith et al. 2015). According to this hypothesis, a lower-than-normal transport from the wGSL could therefore partly explain the negative anomaly of *C. finmarchicus* and the lower abundance (smaller positive anomaly) of *C. hyperboreus* at SV and in the sGSL despite their near-normal or above-normal values in the wGSL and at RS.

In 2014, *C. finmarchicus* showed predominantly negative anomalies for the sixth consecutive year, with abundance being particularly low in the eGSL. This strong negative anomaly in the

eGSL could have resulted from a suite of environmental conditions that were detrimental to the *C. finmarchicus* population. First, the abundance of *C. finmarchicus* was well below its long-term average in 2014 on the Flemish Cap and southeast Grand Banks, an area upstream of Cabot Strait and representing the proximate source for the eGSL population (Maps et al. 2011, DFO 2015). Second, phytoplankton biomass in spring and summer was well below normal in the eGSL, with potentially negative consequences on *C. finmarchicus* productivity under warm conditions such as those that prevailed in the region in summer and fall 2014 (Galbraith et al. 2015). Finally, the massive cohort of the local redfish stock (*Sebastes mentella*) first detected in 2013 was observed again in 2014, with the occurrence of 15–18 cm individuals (2 or 3 years old) in abundances several orders of magnitude greater than the 1990–2012 average in the eGSL (Bourdage et al. 2015). The bulk of this abundance was centred between 150 and 200 m of depth (I. McQuinn, DFO, unpublished data), the overwintering depth of *C. finmarchicus* (Plourde et al. 2001). Given that small redfish (< 25 cm) feed predominantly on large calanoids and other small crustaceans (Gonzalez et al. 2000), it is possible that this new redfish cohort represents a new predatory threat not observed since the early 1980s and strong enough to exert a significant top-down pressure on the GSL *C. finmarchicus* population.

Contrary to 2013, when cold-water copepod species (*C. glacialis*, *M. longa*) showed lower-than-normal abundances across the region, likely in response to warmer-than-normal conditions in all habitats exploited during their life cycle, 2014 was characterized by generally near-normal abundances of cold-water species across the region, i.e., abundances were slightly greater than in 2013. This increase was likely a response to changes in local environmental conditions in 2014, which were probably more favourable than in 2013. Cold-water copepod species could have benefited from a colder-than-normal temperature regime in late fall 2014 and winter 2015 that resulted in an above-normal ice cover (coverage and duration) and a colder CIL (Galbraith et al. 2015). Moreover, higher-than-normal phytoplankton biomass in summer and fall might be beneficial to *M. longa* recruitment: during their fall development, their mesopelagic early copepodite stages can probably exploit sinking phytoplankton aggregates and associated microfauna (Grønvik and Hopkins 1984, Plourde et al. 2002). These environmental conditions might have tempered the adverse effects of warm surface conditions in summer and fall 2014 (Galbraith et al. 2015).

SUMMARY

This document reports on the chemical and biological (plankton) conditions in the GSL in 2014 in the context of a strong warming event initiated in 2010. Data from 2014 are compared to time-series observations.

- The winter maximum nutrient inventories in 2014 showed the first wide-spread positive anomalies since 2007, thus definitively ending the period of strong negative anomalies that was evident in 2010–2011 and to a lesser extent in 2012. This is consistent with the fact that winter conditions were more severe in 2014 relative to the highly anomalous warm conditions generally observed since 2010.
- The shift to earlier timing of the spring bloom observed in recent years was reversed in 2014, with positive (later) anomalies throughout the GSL coinciding with a later-than-normal ice retreat. In addition, the spring bloom magnitude was below normal and of shorter duration across the region.
- The difference between winter (maximum) and late spring (minimum) nitrate inventories was below normal in many regions of the GSL, consistent with lower-than-normal primary production during spring 2014. In fall, chlorophyll *a* levels were nevertheless above normal in many regions of the GSL.

- For a third consecutive year, highly positive deep-water (> 200 m) nitrate concentrations were associated with high temperature and salinity.
- Chlorophyll *a* levels in the St. Lawrence Estuary (weekly sampling at RS) were markedly higher during spring, summer, and fall than were values calculated from satellite images over the rest of the GSL.
- The shift to a smaller-sized phytoplankton community that had been observed in recent years at Rimouski station was reversed in 2014, with positive anomalies in the diatom/flagellate ratios for the first time since 2004. This was largely due to a sharp increase in the relative contribution of diatoms in fall with the concomitant near-disappearance of flagellates, which usually dominate at this time. The trend toward increasing dominance of flagellates at Shediac Valley station continued in 2014, and this was probably associated with warmer conditions observed during summer in the GSL.
- The strong spring freshet of the St. Lawrence River likely impacted the zooplankton community, notably by a lower-than-normal abundance of *C. finmarchicus* and modifications to the phenology of *C. finmarchicus* and *C. hyperboreus* in early summer. Higher food abundance (high phytoplankton biomass at RS and in the wGSL) probably stimulated local zooplankton abundance later in the season.
- The overall high Gulf-wide temperatures (surface and deep layers) and salinities observed in 2014 likely resulted in the well-above-normal (RS, wGSL, eGSL) abundances of warm-water copepod species (*M. lucens*, *Paracalanus* spp., and *Centropages* spp.) as well as the presence of specimens from the family Aetideidae, which was included in the 10 most abundant copepod taxa for the first time this year.
- In the sGSL, water temperatures were near normal in 2014 while phytoplankton biomass was generally greater-than-normal in summer and fall, both of which likely influenced the zooplankton community: copepod species showed near-normal (warm-water spp.) or above-normal (cold-water spp.) abundance anomalies in the sGSL, a signal coherent with the region being cooler than the wGSL and eGSL.
- In 2014, *C. finmarchicus* abundance was generally below normal, particularly in the eGSL, for the sixth consecutive year. This is probably due to unfavourable environmental conditions affecting the copepod's productivity in source regions (e.g., the Newfoundland Shelf), its local food supply (phytoplankton), and predation pressure (presence of a large cohort of redfish (*Sebastes mentella*).
- Abundances of cold-water copepod species (*C. glacialis*, *M. longa*) were generally near normal across the region and higher than in 2013, likely a response to changes in local environmental conditions in 2014 (i.e., colder-than-normal temperatures in late fall 2014 / winter 2015 that resulted in above-normal ice cover and a colder CIL) and an increased food supply. These environmental conditions might have tempered the adverse warm surface conditions in summer and fall 2014.

ACKNOWLEDGEMENTS

We thank Jean-Yves Couture and Sylvie Lessard as well as Isabelle St-Pierre and Caroline Lafleur for preparation and standardization of the phytoplankton and zooplankton data, respectively. The data used in this report would not be available without the work of François Villeneuve and his team (Sylvain Chartrand, Rémi Desmarais, Marie-Lyne Dubé, Yves Gagnon, Line McLaughlin, Roger Pigeon, Daniel Thibault, and the late Sylvain Cantin) in organizing and carrying out AZMP cruises and analyzing samples. Marie-France Beaulieu performed all zooplankton sample analyses. We thank Jeff Spry for providing data from the Shediac Valley station and BIO's remote sensing unit for the composite satellite images. We are grateful to Michael Scarratt for providing comments during the production of this report, and to Catherine Johnson and Pierre Pepin for their critical reviews.

REFERENCES

Arun Kumar, S.V.V., K.N. Babu, and A.K. Shukla. 2015. Comparative analysis of chlorophyll-a distribution from SeaWiFS, MODIS-Aqua, MODIS-Terra and MERIS in the Arabian Sea. Mar. Geod. 38: 40–57.

AZMP. 2006. Physical and biological status of the environment. AZMP Bulletin PMZA 5: 3–8.

Bourdages, H., C. Brassard, M. Desgagnés, P. Galbraith, J. Gauthier, J. Lambert, B. Légaré, E. Parent, and P. Schwab. 2015. Preliminary results from the groundfish and shrimp multidisciplinary survey in August 2014 in the Estuary and northern Gulf of St. Lawrence. DFO Can. Sci. Advis. Sec. Res. Doc. 2014/115. v + 96 p.

Brickman, D., and B. Petrie. 2003. Nitrate, silicate and phosphate atlas for the Gulf of St. Lawrence. Can. Tech. Rep. Hydrogr. Ocean Sci. 231: xi + 152 pp.

de Lafontaine, Y. 1994. Zooplankton biomass in the southern Gulf of St. Lawrence: Spatial patterns and the influence of freshwater runoff. Can. J. Fish. Aquat. Sci. 51(3): 617–635.

DFO. 2015. Oceanographic conditions in the Atlantic zone in 2014. DFO Can. Sci. Advis. Sec. Sci. Advis. Rep. 2015/030.

Ferland, J., M. Gosselin, and M. Starr. 2011. Environmental control of summer primary production in the Hudson Bay system: The role of stratification. J. Mar. Syst. 88(3): 385–400.

Galbraith, P. S. 2006. Winter water masses in the Gulf of St. Lawrence. J. Geophys. Res. 111, C06022, doi:10.1029/2005JC003159.

Galbraith, P. S., R. Desmarais, R. Pigeon, and S. Cantin. 2006. Ten years of monitoring winter water masses in the Gulf of St. Lawrence by helicopter. AZMP Bulletin PMZA 5: 32–35.

Galbraith, P. S., J. Chassé, D. Gilbert, P. Larouche, C. Caverhill, D. Lefaivre, D. Brickman, B. Pettigrew, L. Devine, and C. Lafleur. 2014. Physical oceanographic conditions in the Gulf of St. Lawrence in 2013. DFO Can. Sci. Advis. Sec. Res. Doc. 2014/062. vi + 84 pp.

Galbraith, P. S., J. Chassé, P. Nicot, C. Caverhill, D. Gilbert, B. Pettigrew, D. Lefaivre, D. Brickman, L. Devine, and C. Lafleur. 2015. Physical oceanographic conditions in the Gulf of St. Lawrence in 2014. DFO Can. Sci. Advis. Sec. Res. Doc. 2015/032. v+82 pp.

Gonzalez, C., I. Bruno, and X. Paz. 2000. Food and feeding of deep-sea redfish (*Sebastes mentella* Travin) in the North Atlantic. NAFO Sci. Coun. Studies 33: 89–101.

Gregg, W. W., and C. S. Rousseaux. 2014. Decadal trends in global pelagic ocean chlorophyll: A new assessment integrating multiple satellites, in situ data, and models. J. Geophys. Res. Oceans, 119: 5921–5933, doi 10.1002/2014JC010158.

Grønvik, S., and C. C. E. Hopkins.1984. Ecological investigations of the zooplankton community of Balsfjorden, northern Norway: Generation cycle, seasonal vertical distribution, and seasonal variations in body weight and carbon and nitrogen content of the copepod *Metridia longa* (Lubbock). J. Exp. Mar. Biol. Ecol. 80: 93–107.

Le Fouest, V., B. Zakardjian, F. Saucier, and M. Starr. 2005. Seasonal versus synoptic variability in planktonic production in a high-latitude marginal sea: the Gulf of St. Lawrence (Canada). J. Geophys. Res. 110, C09012, doi 10.1029/2004JC002423.

Le Fouest, V., B. Zakardjian, and F. J. Saucier. 2010. Plankton ecosystem response to freshwater-associated bulk turbidity in the subarctic Gulf of St. Lawrence (Canada): A modelling study. J. Mar. Syst. 81(1-2): 75–85.

Levasseur, M., J.-C. Therriault, and L. Legendre. 1984. Hierarchical control of phytoplankton succession by physical factors. Mar. Ecol. Prog. Ser. 19: 211–222.

Li, W. K. W., and W. G. Harrison. 2008. Propagation of an atmospheric climate signal to phytoplankton in a small marine basin. Limnol. Oceanogr. 53(5): 1734–1745.

Maps, F., B. Zakardjian, S. Plourde, and F.J. Saucier. 2011. Modeling the interactions between the seasonal and diel migration behaviors of *Calanus finmarchicus* and the circulation in the Gulf of St. Lawrence (Canada). J. Mar. Syst. 88: 183–202.

Mei, Z.-P., F. Saucier, V. Le Fouest, B. Zakardjian, S. Sennville, H. Xie, and M. Starr. 2010. Modeling the timing of spring phytoplankton bloom and biological production of the Gulf of St. Lawrence (Canada): Effects of colored dissolved organic matter and temperature. Cont. Shelf Res. 30: 2027–2042.

Mitchell, M. R., G. Harrison, K. Pauley, A. Gagné, G. Maillet, and P. Strain. 2002. Atlantic Zonal Monitoring Program sampling protocol. Can. Tech. Rep. Hydrogr. Ocean Sci. 223: iv + 23 pp.

Mucci, A., M. Starr, D. Gilbert, and B. Sundby. 2011. Acidification of lower St. Lawrence Estuary bottom waters. Atmos.-Ocean 49(3): 206–218.

Plourde, S., P. Joly, J. A. Runge, B. Zakardjian, and J. J. Dodson. 2001. Life cycle of *Calanus finmarchicus* in the lower St. Lawrence Estuary: imprint of circulation and late phytoplankton bloom. Can. J. Fish. Aquat. Sci. 58: 647–658.

Plourde, S., J. J. Dodson, J. A. Runge, and J.-C. Therriault. 2002. Spatial and temporal variations in copepod community structure in the lower St. Lawrence Estuary, Canada. Mar. Ecol. Prog. Ser. 230: 221–224.

Plourde, S., F. Maps, and P. Joly. 2009. Mortality and survival in early stages control recruitment in *Calanus finmarchicus*. J. Plankton Res. 31(4): 371–388.

Plourde, S, M. Starr, L. Devine, J.-F. St-Pierre, L. St-Amand, P. Joly, and P. S. Galbraith. 2014. Chemical and biological oceanographic conditions in the Estuary and Gulf of St. Lawrence during 2011 and 2012. DFO Can. Sci. Advis. Sec. Res. Doc. 2014/049. v + 46 pp.

Runge, J. A., M. Castonguay, Y. de Lafontaine, M. Ringuette, and J.-L. Beaulieu. 1999. Covariation in climate, zooplankton biomass and mackerel recruitment in the southern Gulf of St Lawrence. Fish. Oceanogr. 8: 139–149.

Therriault, J.-C., and M. Levasseur. 1985. Control of phytoplankton production in the Lower St. Lawrence Estuary: light and freshwater runoff. Nat. Can. 112: 77–96.

Therriault, J.-C., B. Petrie, P. Pépin, J. Gagnon, D. Gregory, J. Helbig, A. Herman, D. Lefaivre, M. Mitchell, B. Pelchat, J. Runge, and D. Sameoto. 1998. Proposal for a Northwest Atlantic zonal monitoring program. Can. Tech. Rep. Hydrogr. Ocean Sci. 194: vii + 57 pp.

Zakardjian, B. A., Y. Gratton, and A. F. Vézina. 2000. Late spring phytoplankton bloom in the Lower St. Lawrence Estuary: the flushing hypothesis revisited. Mar. Ecol. Prog. Ser. 192: 31–48.

Zhai, L., T. Platt, C. Tang, S. Sathyendranath, and R. Hernández Walls. 2011. Phytoplankton phenology on the Scotian Shelf. ICES J. Mar. Sci. 68: 781–791 (doi:10.1093/icesjms/fsq175).

Zibordi, G., F. Mélin, and J.-F. Berthon. 2006. Comparison of SeaWiFS, MODIS and MERIS radiometric products at a coastal site. Geophys. Res. Letters, 33, L06617, doi:10.1029/2006GL025778.

TABLES

Table 1. List of AZMP missions with locations, dates, and sampling activities for 2014. wGSL, eGSL, and sGSL denote the western, eastern, and southern subregions of the Gulf of St. Lawrence. See Figure 1 for station locations.

Sampling group	Name	Location	Dates	Vessel	Hydro	Net
Fixed	Rimouski	48º40.0'N/068º35.0'W	22 APR-16 DEC	Beluga II	29	26
	Shediac Valley	47º46.8'N/064º01.8'W	18 MAR-06 NOV	Multiple	8	7
Total					37	33
Sections Spring	TESL	wGSL	31 MAY-11JUN	Hudson	7	5
	TSI	wGSL	31 MAY-11JUN	Hudson	6	6
	TASO	wGSL	31 MAY-11JUN	Hudson	5	4
	TIDM	sGSL	31 MAY-11JUN	Hudson	10	10
	TDC	eGSL	31 MAY-11JUN	Hudson	6	6
	TCEN	eGSL	31 MAY-11JUN	Hudson	5	5
	TBB	eGSL	31 MAY-11JUN	Hudson	7	7
Total					46	43
Sections Fall	TESL	wGSL	27 OCT-11 NOV	Hudson	7	7
	TSI	wGSL	27 OCT-11 NOV	Hudson	6	6
	TASO	wGSL	27 OCT-11 NOV	Hudson	5	5
	TIDM	sGSL	27 OCT-11 NOV	Hudson	10	10
	TDC	eGSL	27 OCT-11 NOV	Hudson	6	6
	TCEN	eGSL	27 OCT-11 NOV	Hudson	5	5
	TBB	eGSL	27 OCT-11 NOV	Hudson	7	7
Total					46	46

FIGURES

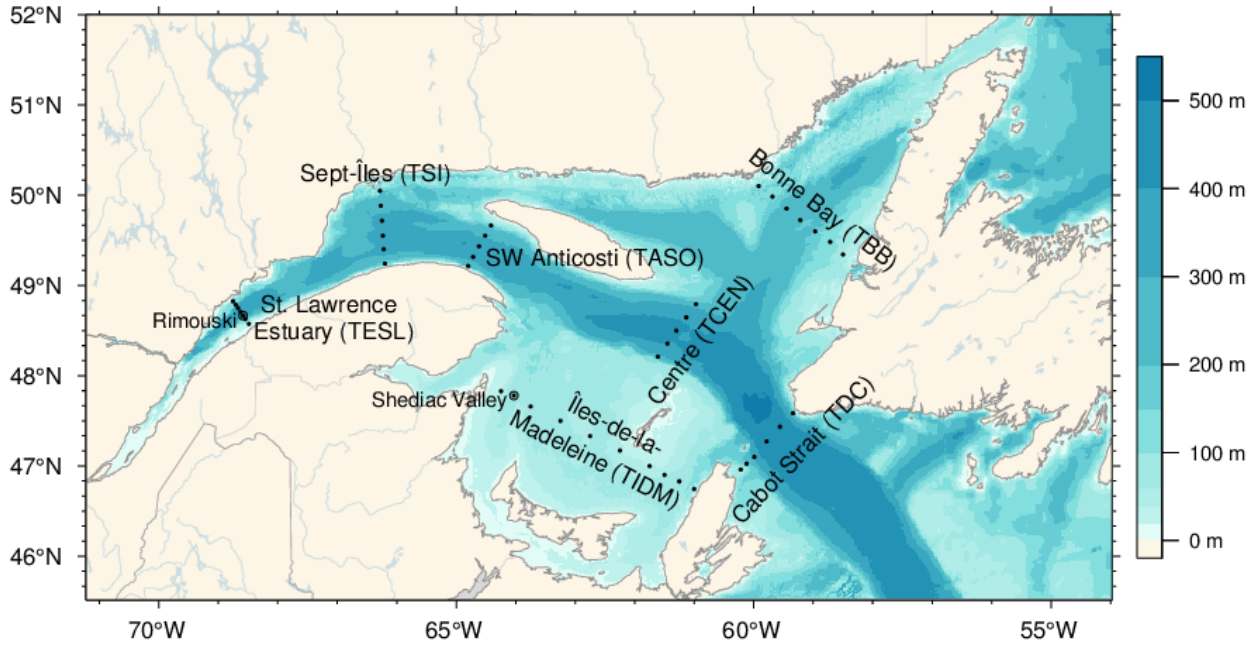

Figure 1. Bathymetric map of the Estuary and Gulf of St. Lawrence showing sampling stations on the different sections (dots) and at Rimouski and Shediac Valley stations (circles). Sections were grouped to form subregions: TESL, TSI, TASO: western GSL; TIDM: southern GSL; TBB, TCEN, TDC: eastern GSL.

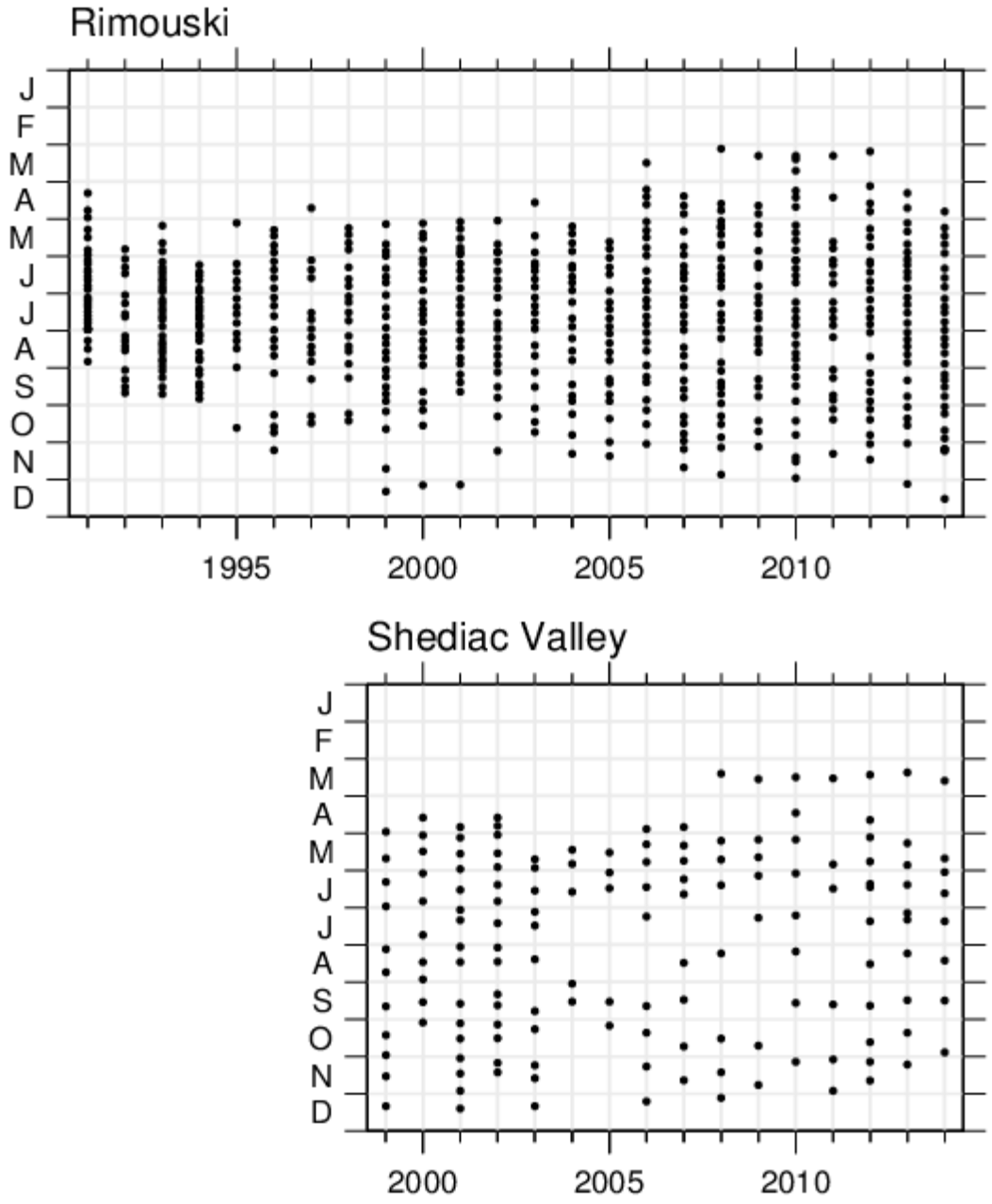

Figure 2. Sampling frequencies at Rimouski and Shediac Valley stations showing bottle and net sampling effort through 2014.

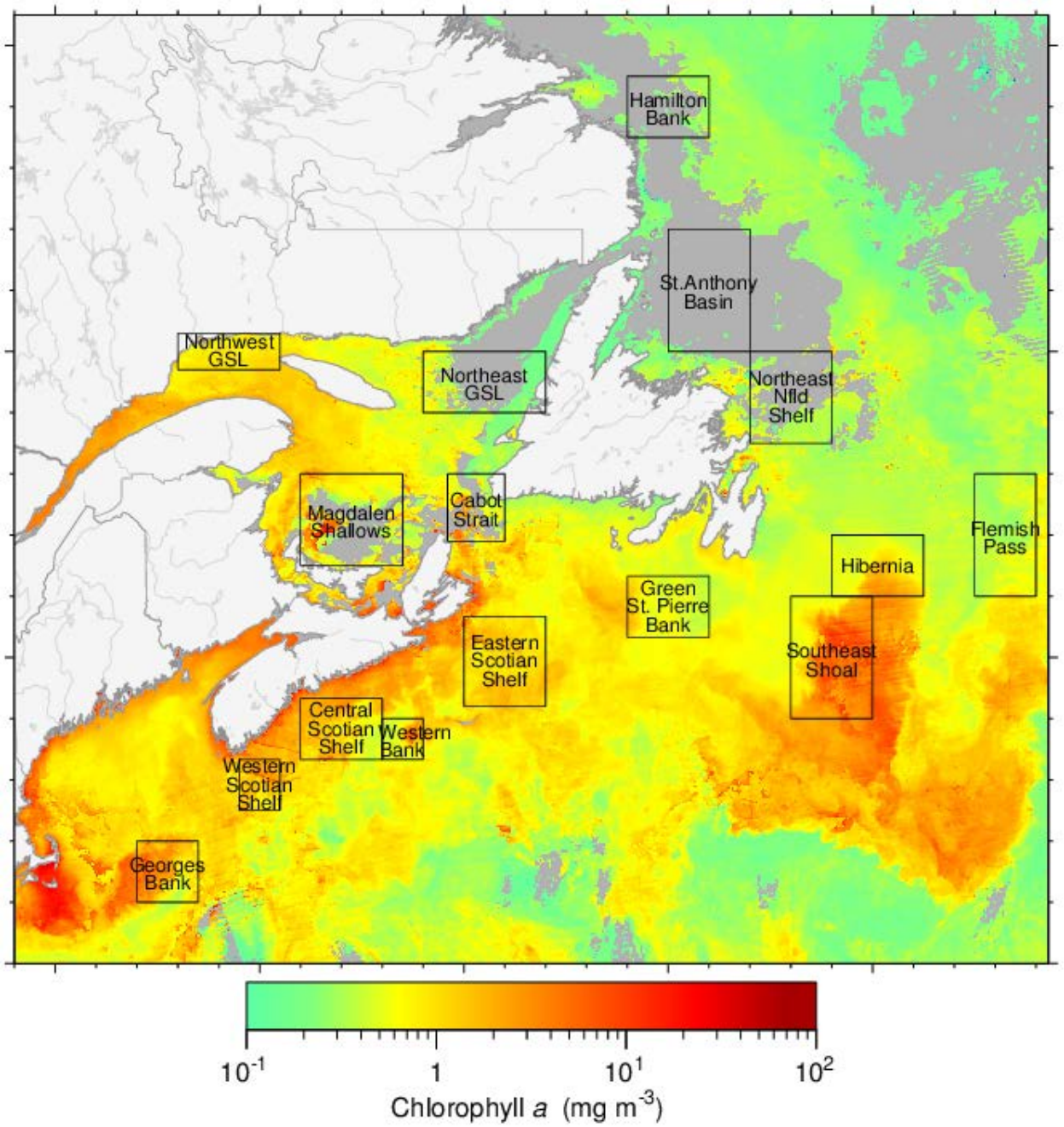

Figure 3. Statistical subregions in the Northwest Atlantic identified for spatial/temporal analysis of satellite ocean colour data. Only the Gulf of St. Lawrence (GSL) subregions are discussed in this report (Northwest GSL, Northeast GSL, Magdalen Shallows, Cabot Strait). The figure is a MODIS composite image showing chlorophyll a from 1–15 April 2014. Gray areas indicate no data (in this case because of ice; near-shore regions are also excluded).

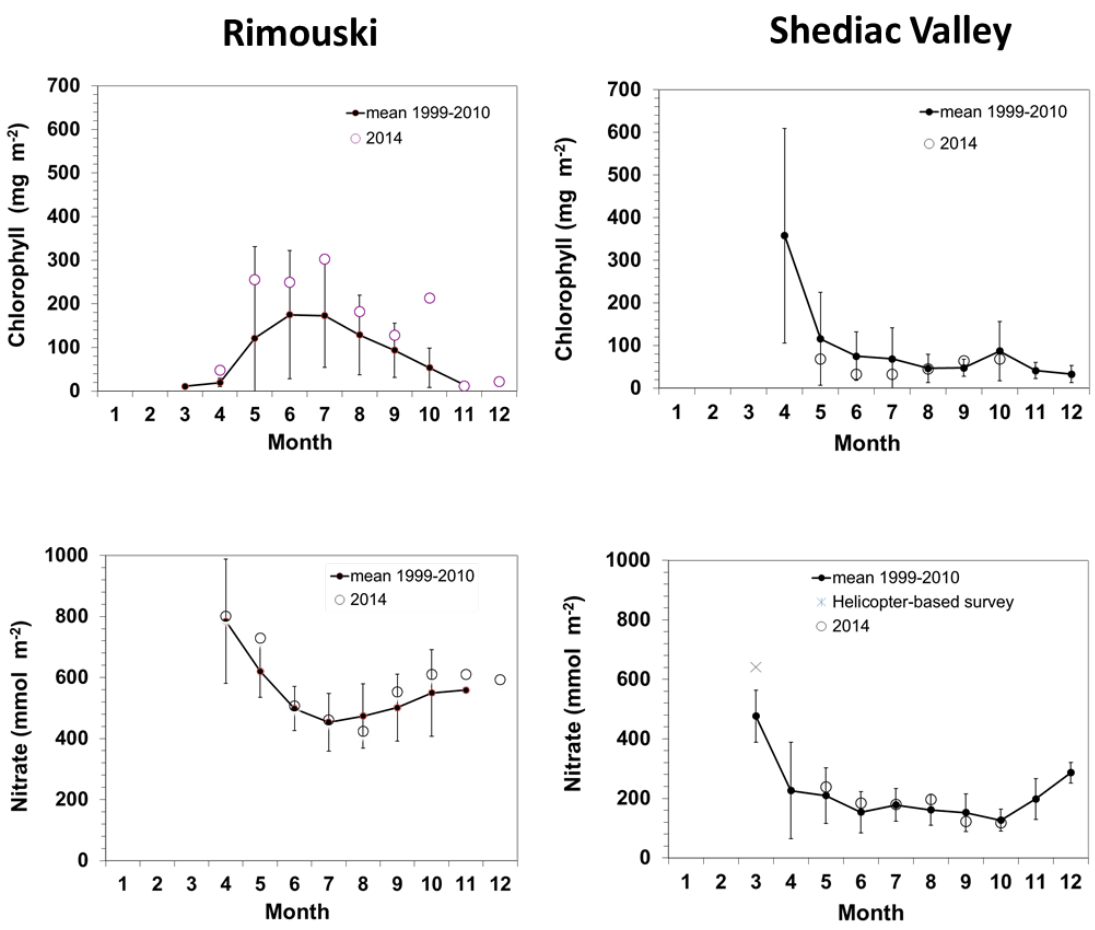

Index	Station	1999	2000	2001	2002	2003	2004	2005	2006	2007	2008	2009	2010	2011	2012	2013	2014	Mean	S.D.
Nitrate 0-50 m	RS	-0.35	0.61	0.07	1.13	-0.30	0.85	-0.29	0.00	-0.07	0.43	-0.44	-1.32	-0.62	-0.28	0.08	0.28	554	115
(mmol m^{-2})	SV	0.23	0.66	-0.32	0.16	0.16	0.55	-0.23	0.66	-1.15	-0.09	0.66	-1.16	-0.85	0.18	-0.40	0.12	188	71
Nitrate 50-150 m	RS		-0.27	0.54	0.95	-0.68	-0.12	-0.26	0.61	0.67	-0.39	0.18	-1.18	-1.06	0.14	-0.73	0.96	1471	45
(mmol m^{-2})	SV	-0.15	1.01	0.17	0.67	-0.06	0.53	-0.17	0.61	-1.17	0.12	-0.09	-1.39	-1.50	-0.43	-0.96	-0.44	275	65
Chlorophyll 0-100 m	RS	1.71	-0.23	0.04	-0.26	0.48	-0.76	-0.41	-0.47	0.50	-0.89	0.24	0.02	-0.28	0.55	0.13	1.39	109	58
(mg m^{-2})	SV	-0.44	-0.70	-0.26	1.13	0.23	-0.46	-0.56	-0.13	0.46	0.60	0.14	-0.25	-0.65	-0.09	0.73	-0.19	97	73

Figure 4. Chlorophyll levels (0–100 m; top panels) and nitrate inventories (0–50 m; bottom panels) in 2014 (open circles) with mean conditions from 1999–2010 (dots and solid line) at Rimouski (RS) and Shediac Valley (SV) stations. Vertical lines are the 95% confidence intervals of the monthly mean. Early winter nitrate values are from the March helicopter survey (samples from 2 m). Normalized annual anomalies (scorecard) for nutrient inventories (mmol m^{-2}) and chlorophyll levels (mg m^{-2}) are also presented with the variables' means and standard deviations. Blue colours indicate anomalies below the mean and reds are anomalies above the mean.

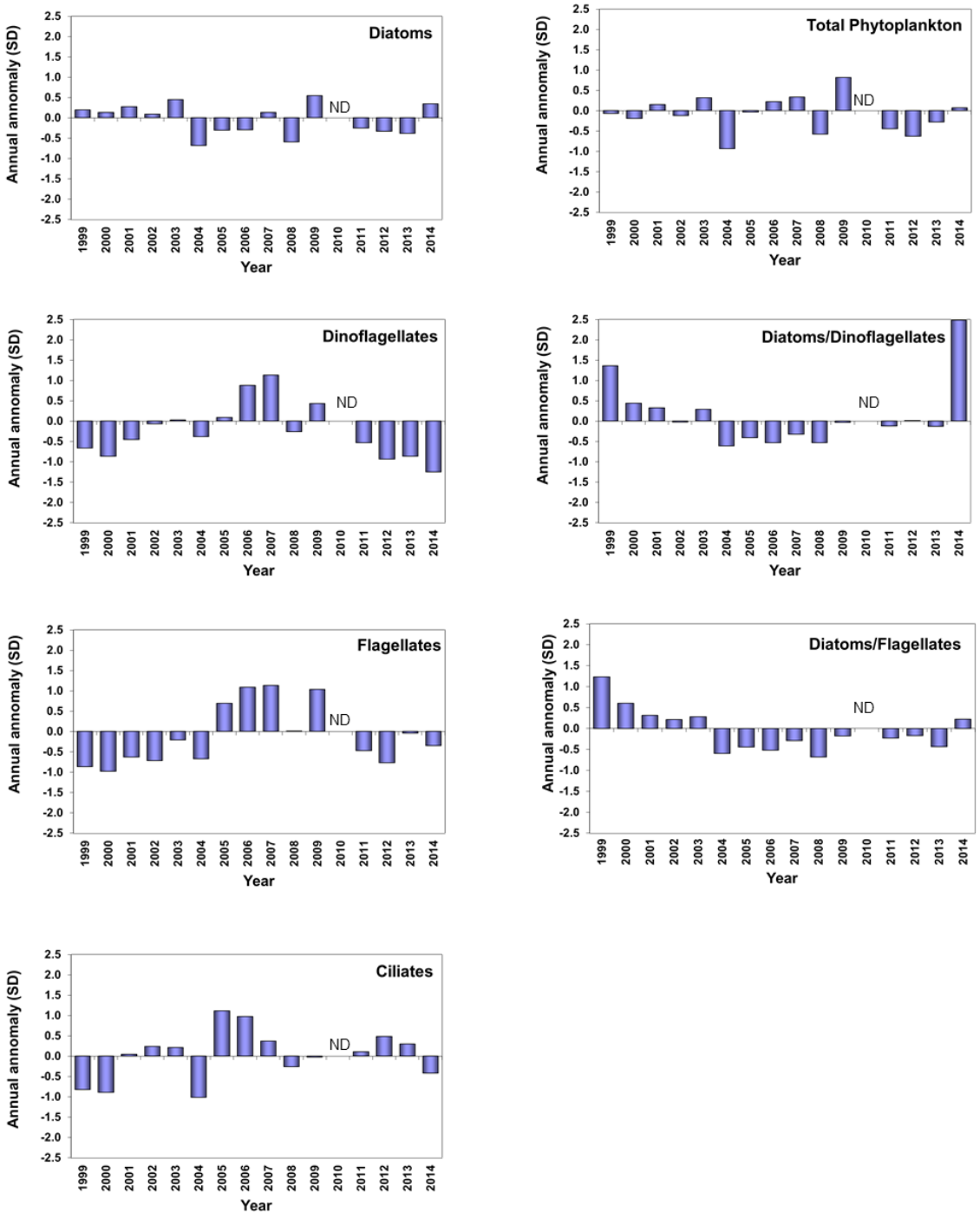

Figure 5. Time series of microplankton abundance anomalies for total phytoplankton and by group (diatoms, dinoflagellates, flagellates, ciliates), and for the diatom/dinoflagellate and diatom/flagellate ratios at Rimouski station, 1999–2014 (no data for 2010).

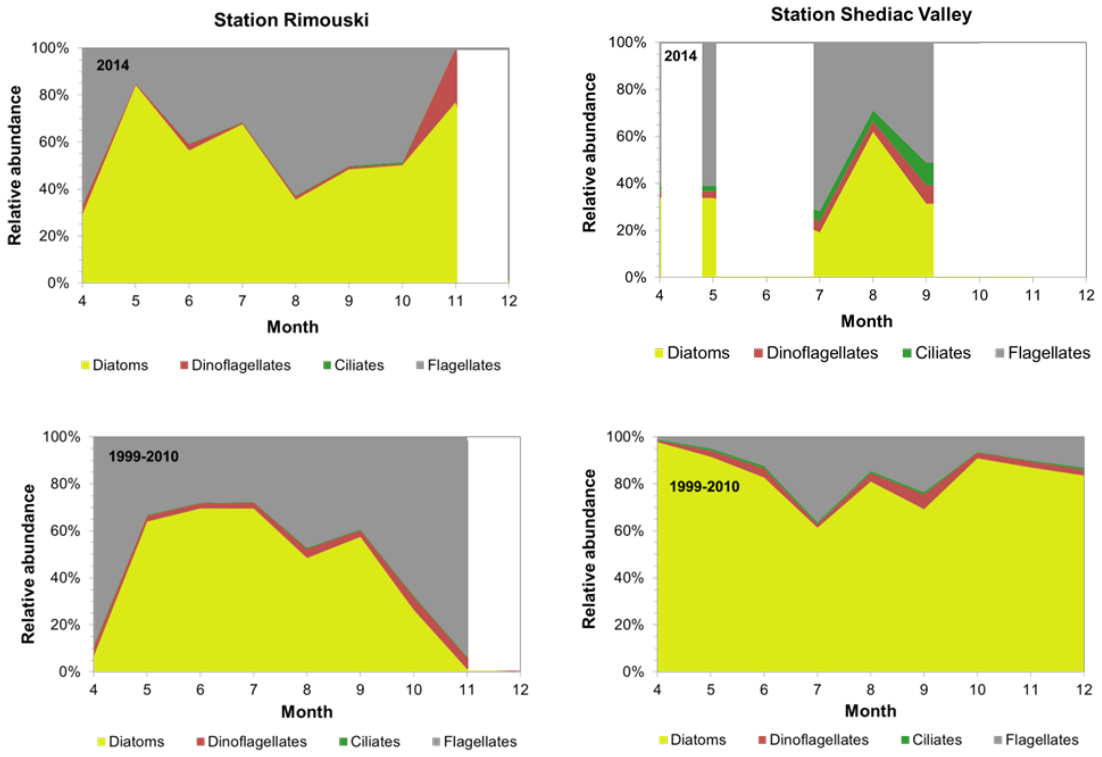

Figure 6. Phytoplankton community composition at Rimouski and Shediac Valley stations for 2014 (top panels) and for the 1999–2010 average (bottom panels). (The ciliate group is shown between the dinoflagellate and flagellate groups on the figures; it is usually so scarce that it is barely visible.) Note that phytoplankton was analyzed on four occasions only for SV (May, July–Sept).

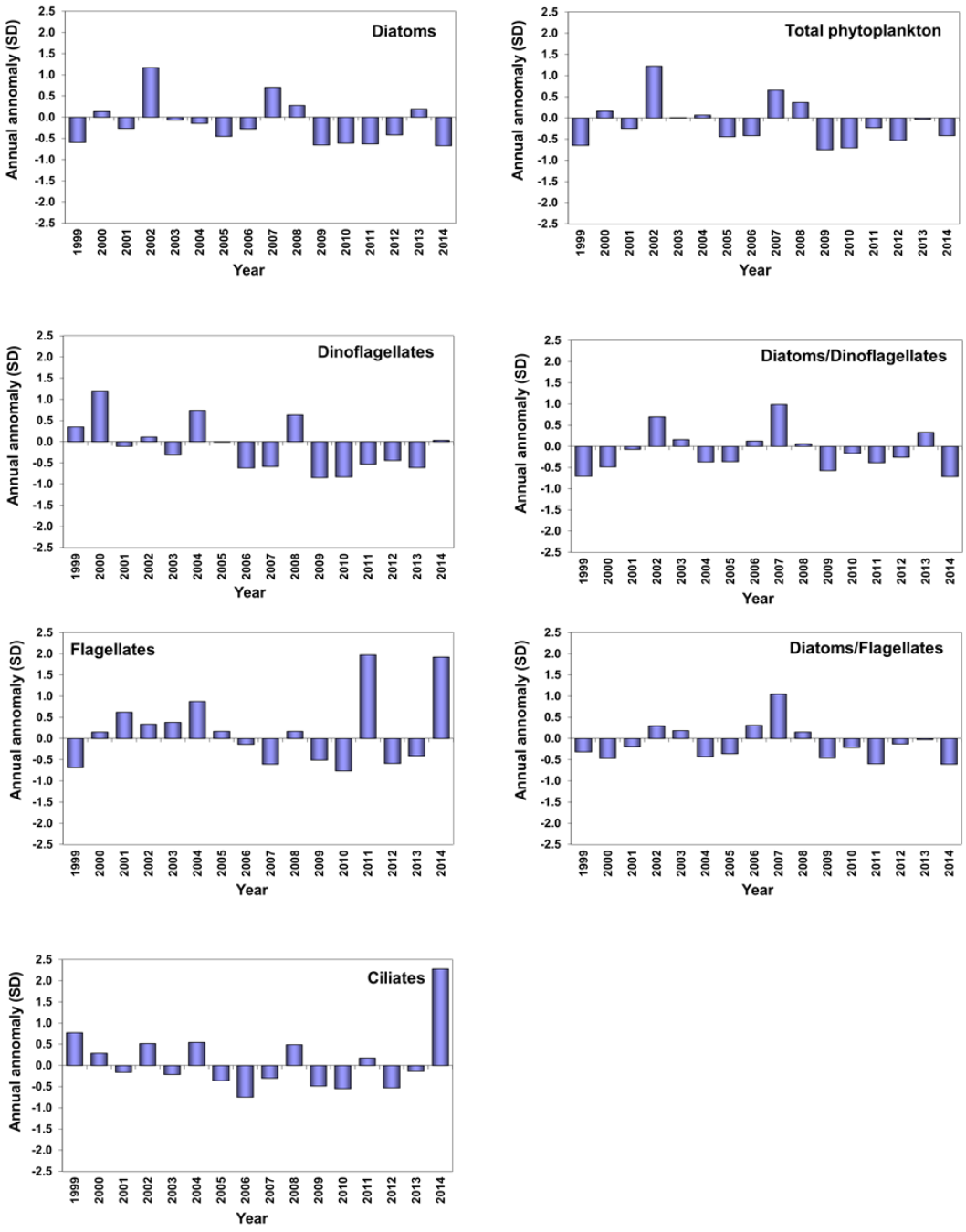

Figure 7. Time series of microplankton abundance anomalies for total phytoplankton and by group (diatoms, dinoflagellates, flagellates, ciliates), and for the diatom/dinoflagellate and diatom/flagellate ratios at Shediac Valley station, 1999–2014.

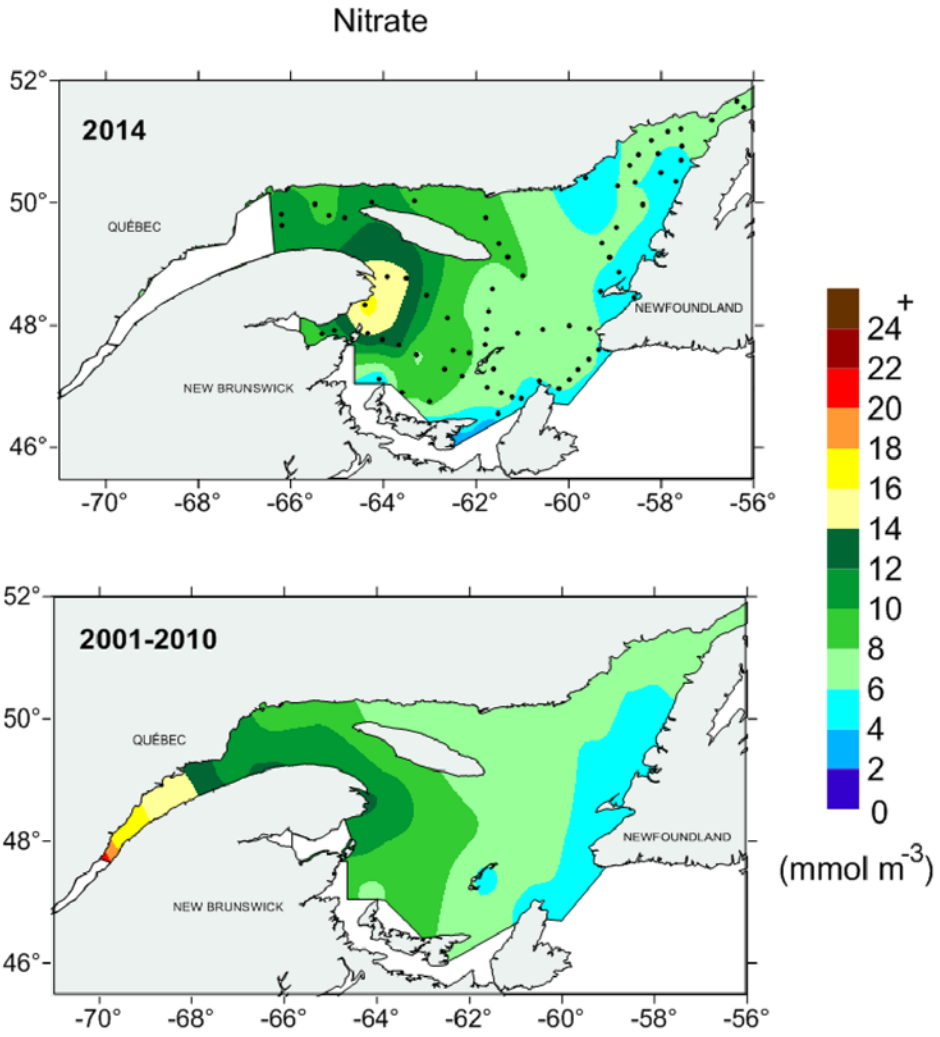

Figure 8. Nitrate concentrations (mmol m^{-3}) at 2 m collected in the Estuary and Gulf of St. Lawrence during the helicopter survey in late winter (mid-March) 2014 compared to the 2001–2010 average. Dots indicate sampling locations.

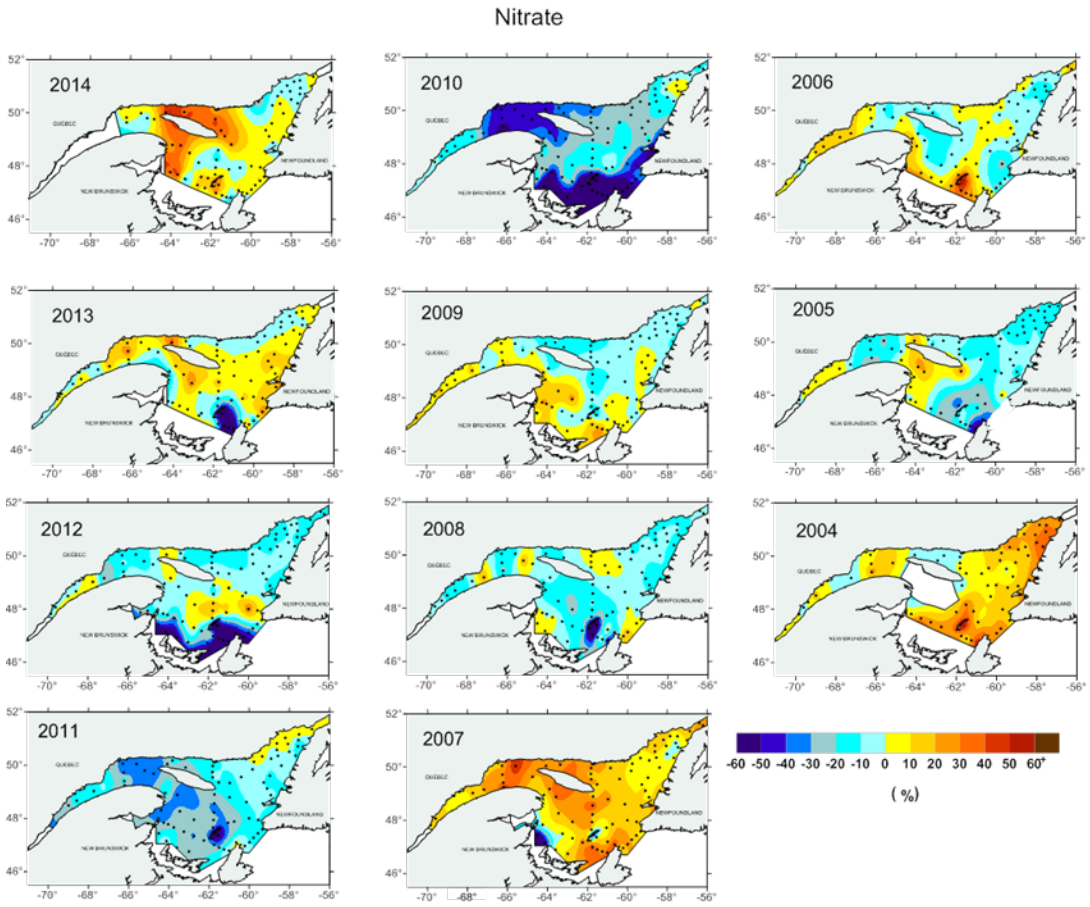

Figure 9. Percentage of change in the late winter (mid-March) nitrate concentrations at 2 m from samples collected during the helicopter survey from 2004 to 2014 relative to the 2001–2010 average. Dots indicate sampling locations.

Index	Transect	1999	2000	2001	2002	2003	2004	2005	2006	2007	2008	2009	2010	2011	2012	2013	2014	Climatology Mean	S.D.	%
Winter nitrate inventory (0-50m	TESL			-0.33	-0.62	0.86	0.59		1.49	0.71	-1.51	0.19	-1.53	-1.72	-0.17	0.35		770	85	
(mmol m^{-2})	TSI			-0.13	0.35	1.24	0.54	-0.76	0.02	1.26	-0.73	0.25	-2.06	-1.22	-0.43	0.54	-0.12	528	125	-3
	TASO			-0.23	0.05	1.21	-0.07	0.05	0.33	1.04	-0.15	0.25	-2.49	-1.85	-0.36	-0.44	0.90	522	89	15
	TCEN			-0.65	-0.26	1.92	0.80	-0.94	-0.10	1.33	-0.62	-0.60	-0.89	-1.45	0.25	0.37	0.28	344	51	4
	TBB			-0.33	0.28	1.90	0.95	-0.72	-0.16	0.55	-0.70	-0.05	-1.72	-0.49	-0.63	0.52	-0.12	299	38	-2
	TIDM			-0.02	0.44	0.58	0.91	-0.52	0.83	0.55	-0.76	0.38	-2.38	-0.93	-1.34	-0.84	0.55	384	99	14
	TDC			0.40	0.16	1.31	0.79	-0.98	-0.39	0.69	0.19	0.03	-2.20	-0.37	-1.02	0.15	0.14	293	80	4
Spring nitrate inventory (0-50m)	TESL			0.01	1.67	-0.23	0.43		1.26	-0.79	-0.03	-0.95	-1.37	-0.58	0.23	1.61	1.62	437	92	34
(mmol m^{-2})	TSI	-1.21	-0.05	0.99	1.39	1.16	-0.70	-0.58	-0.02	-0.90	1.51	-0.59	-1.00	-1.04	-0.70	1.33	2.65	203	46	60
	TASO	-1.55	-0.62	-0.20	1.22	1.71	0.48	-0.67	-0.78	0.82	0.56	0.22	-1.20	-0.97	-1.26	1.46	2.91	186	59	93
	TCEN						-1.53	-0.01	0.96	-0.04	1.35	0.22	-0.95	-0.85	-1.62	2.55	4.35	68	20	125
	TIDM	-0.84	1.03	-0.83	-0.23	0.27	-0.62	-0.24	1.68	0.00	1.05	0.63	-1.91	-0.52	-0.99	0.89	0.39	109	38	14
	TBB	-0.33	0.34	-0.33	-0.30	2.50	-1.37	-0.96	-0.09	0.70	0.75	-0.59	-0.31	-1.13	-0.81	-1.30	2.05	63	24	78
	TDC	-1.22	0.96	-0.24	-1.45	0.79	-0.12	-0.98	0.03	0.57	2.07	0.04	-0.45	-1.53	-0.69	-0.09	0.49	71	21	15
Difference between winter	TESL			-0.25	-1.86	0.87	0.11		0.12	1.22	-1.14	0.95	-0.03	-0.83	-0.31	-1.06		332	111	
and late spring nitrate inventory	TSI			-0.44	-0.11	0.86	0.84	-0.50	0.10	1.63	-1.23	0.51	-1.64	-0.79	-0.13	0.10	-1.03	319	126	-41
(0-50m)	TASO			0.07	-0.84	0.29	-0.33	0.87	1.35	0.87	-0.51	0.33	-2.09	-1.43	0.85	-1.71	-1.21	323	65	-25
(mmol m^{-2})	TCEN						1.45	-0.75	-0.30	1.41	-0.94	-0.51	-0.36	-0.93	0.97	-0.44	-1.18	269	54	-24
	TIDM			0.35	0.61	0.55	1.34	-0.51	0.20	0.63	-1.38	0.15	-1.94	-0.86	-1.13	-1.40	0.46	275	84	14
	TBB			-0.13	0.51	0.36	1.98	-0.13	-0.11	0.12	-1.28	0.36	-1.68	0.23	-0.14	1.47	-1.54	236	35	-23
	TDC			0.50	0.59	1.19	0.89	-0.77	-0.42	0.58	-0.37	0.03	-2.22	0.04	-0.89	0.20	0.02	221	75	1
Fall nitrate inventory (0-50m)	TESL	2.49	-0.11	0.46	1.12	-0.61	-1.10	0.28	-0.78	-0.76	-0.07	-0.58	-0.33	-0.06	0.70	-0.45	-0.10	534	116	-2
(mmol m^{-2})	TSI	1.91	-0.73	1.06	1.23	0.50	-1.28	-1.15	-0.32	-0.71	-0.49	-0.27	0.27	-0.46	1.57	0.71	-0.08	268	102	-3
	TASO	1.89	-0.29	0.86	1.19	-1.18	-1.04	-0.64	-0.34	-0.59	0.37	-1.03	0.81	-1.01	1.34	-0.01	0.72	278	74	19
	TCEN					-0.05	-0.91	-0.37	-0.25	2.09	0.17	0.47	-1.15	-2.83	-1.95	-1.10	-0.81	136	28	-17
	TIDM		1.17	0.59	-0.04	-1.25	1.31	0.14	1.35	-0.93	-0.22	-0.91	-1.20	-2.15	-1.35	-0.19	-0.61	183	36	-12
	TBB	0.94	0.33	1.27	0.12	0.79	-1.88	-0.29	-1.62	1.00	-0.38	0.24	-0.54	-0.51	-1.50	-0.97	-1.37	125	31	-33
	TDC	1.44	0.73	-0.16	2.19	-0.59	-1.29	0.08	-0.11	-0.54	-0.61	-0.24	-0.91	-1.02	-0.50	0.12	-1.16	135	45	-39
Seasonally adjusted nitrate	TESL	2.60	0.09	0.02	0.97	-0.59	-0.58	0.47	-0.10	-0.88	-0.25	-0.85	-0.89	-0.46	0.21	0.19	0.37	511	120	9
inventory (0-50m)	TSI	1.16	-0.64	1.27	1.56	0.86	-1.35	-1.20	-0.28	-0.94	0.16	-0.45	-0.15	-0.78	1.06	1.10	0.93	235	60	24
(mmol m^{-2})	TASO	0.66	-0.80	0.72	2.23	0.20	-0.67	-1.21	-1.00	0.07	0.84	-0.88	-0.15	-1.84	0.34	1.19	3.13	232	36	48
	TCEN					1.25	-1.42	-0.42	0.07	1.11	0.51	0.21	-1.31	-2.32	-2.10	0.24	1.20	106	23	26
	TIDM	-1.82	1.28	-0.02	-0.02	-0.37	0.46	0.07	1.72	-0.35	0.58	0.00	-1.52	-1.26	-1.10	0.51	0.02	142	36	1
	TBB	0.45	0.39	0.67	-0.08	1.82	-1.95	-0.69	-1.11	1.02	0.14	-0.14	-0.52	-0.92	-1.41	-1.32	0.16	94	23	4
	TDC	1.03	1.37	-0.32	1.78	-0.26	-1.58	-0.43	-0.12	-0.32	0.41	-0.26	-1.31	-2.02	-0.96	0.09	-1.09	103	19	-21
Seasonally adjusted nitrate	TESL			1.04	1.56	0.18	-1.31		0.48	-0.04	-0.45	0.06	-1.52	-1.16	1.03	0.54	0.81	1336	110	7
inventory (50-150m)	TSI	0.03	-1.39	0.73	1.24	0.95	-1.38	-0.87	0.68	-0.18	1.34	-1.07	-0.09	-0.50	1.09	0.61	0.23	1354	144	2
(mmol m^{-2})	TASO	-0.05	-1.53	0.20	1.36	0.89	-0.98	-1.00	1.01	-0.08	1.06	0.43	-1.31	-0.50	2.18	0.39	2.51	1256	100	20
	TCEN						-1.52	-0.28	1.19	0.69	0.31	0.68	-1.08	-0.91	-0.33	0.97	0.16	1093	106	2
	TIDM																			
	TBB	-2.58	-0.17	-0.05	0.48	1.08	-1.03	-0.06	0.93	0.72	0.13	-0.12	0.67	0.42	0.40	0.60	0.54	898	99	6
	TDC	-1.07	1.90	-1.30	-0.01	0.27	-1.14	-0.62	1.51	-0.30	0.52	0.35	-0.10	-0.53	1.83	0.64	1.03	867	86	10
Seasonally adjusted nitrate	TESL	2.49	-0.67	-0.35	0.14	-0.40	-0.20	0.48	0.77	-0.69	-0.04	-1.64	0.10	-0.56	0.24	0.31	0.42	23.9	1.5	2.6
inventory (300m)	TSI	-2.20	-1.32	-0.16	0.84	1.07	-0.49	-0.36	1.19	0.48	0.70	0.19	0.05	0.40	1.52	2.58	2.12	23.5	0.8	7.1
(mmol m^{-3})	TASO	-0.52	-0.39	-2.17	0.52	-0.05	0.77	0.78	0.19	-1.55	0.84	0.82	0.76	-0.94	1.36	2.33	2.57	23.4	0.6	6.6
	TCEN						-0.72	0.04	0.76	0.06	1.37	0.21	-1.72	0.26	2.33	3.81	3.82	21.9	0.4	7.3
	TDC	-1.36	0.81	-0.18	-1.76	1.55	-0.13	-0.58	0.92	-0.32	0.12	-0.31	1.25	-1.96	1.42	1.92	2.30	21.3	0.7	7.2

Spring chlorophyll concentration	TESL		0.00	0.97	-0.93	1.65	-0.91	0.00	-0.97	1.10	-0.66	-0.07	-0.19	-0.40	-0.10	-1.22	0.10	148	97	6
(0-100m)	TSI	-0.18	-1.35	0.08	2.29	-0.34	1.32	-0.82	0.28	0.21	-0.90	-0.66	0.08	-0.25	0.46	-1.23	-0.23	69	38	-13
(mg Chl m^{-2})	TASO	-0.43	-0.68	-0.73	2.79	-0.38	0.54	0.50	0.38	-0.71	-0.60	-0.56	-0.13	-0.55	-0.12	-0.98	-0.38	94	67	-27
	TCEN						-0.84	-0.62	-0.74	0.63	1.73	0.62	-0.77	-0.84	-0.94	-0.02	-0.79	38	12	-25
	TIDM	-0.20	-1.56	-0.51	2.41	0.27	-0.07	-0.72	-0.01	-0.21	-0.45	-0.21	1.25	-0.20	-0.25	0.56	-0.02	36	14	-1
	TBB	-0.96	0.47	-1.16	1.64	-0.81	1.74	-0.66	-0.84	-0.13	0.81	-0.46	0.35	-1.06	-0.43	1.61	-0.36	29	11	-13
	TDC	2.01	-0.62	-0.01	2.10	-0.68	-0.73	-0.74	-0.12	-0.45	-0.50	-0.36	0.08	-0.47	-0.41	-0.44	0.24	47	32	17
Fall chlorophyll concentration	TESL	-0.71	-1.63	-0.64	-0.12	1.20	0.18	-0.29	-0.07	0.02	2.41	-0.23	-0.12	-0.41	0.73	-0.96	0.67	23	9	26
(0-100m)	TSI	-0.45	-0.86	-0.57	-0.19	0.26	-0.26	0.41	-0.32	-0.24	2.98	-0.52	-0.25	-0.54	-0.29	-0.51	-0.17	46	34	-13
(mg Chl m^{-2})	TASO	-0.57	-0.95	-0.55	-0.17	0.64	-0.52	0.23	-0.12	-0.19	2.89	-0.14	-0.54	-0.27	0.11	-0.01	-0.20	45	32	-14
	TCEN					1.29	-1.41		-0.87	-0.57	0.20	0.31	1.06	-1.48	0.00	-0.20	1.77	42	8	35
	TIDM		-1.64	0.59	1.71	0.79	-0.85	-0.85	-0.44	1.22	-0.50	-0.12	0.09	0.48	1.67	2.12	0.98	38	13	34
	TBB	-0.58	-1.36	-0.27	1.37	1.01	2.09	-0.60	-0.72	0.26	-0.59	-0.22	-0.38	0.99	0.78	0.40	1.24	35	11	38
	TDC	-0.91	-1.70	-0.24	1.53	0.35	-0.30	-0.82	0.79	1.07	-0.45	1.29	-0.61	-0.76	-0.66	1.11	1.47	41	11	40
Seasonally adjusted chlorophyll	TESL	-1.01	-1.16	1.16	-0.53	1.93	-0.49	-0.94	-0.56	1.33	-0.08	0.23	0.14	-0.08	0.28	-0.89	0.46	69	53	35
concentration (0-100m)	TSI	-0.49	-1.80	-0.36	1.80	-0.10	0.93	-0.38	-0.01	0.00	1.48	-0.96	-0.12	-0.62	0.17	-1.43	-0.32	58	22	-13
(mmol m^{-2})	TASO	-0.66	-1.06	-0.93	2.55	-0.08	0.28	0.57	0.30	-0.75	0.73	-0.59	-0.36	-0.64	-0.06	-0.92	-0.44	69	36	-23
	TCEN						-1.22	-1.04	-0.91	0.14	1.21	0.53	-0.05	-1.25	-0.65	-0.12	0.26	40	9	6
	TIDM	-0.54	-1.48	-0.74	0.89	0.34	-0.24	0.05	-0.23	-0.39	2.52	-0.56	0.38	-0.57	-0.29	-0.15	-0.25	37	16	-11
	TBB	-0.87	-0.54	-0.80	1.72	0.15	2.20	-0.72	-0.90	0.08	0.10	-0.38	-0.03	-0.03	0.21	1.15	0.52	32	9	15
	TDC	1.51	-1.08	-0.08	2.35	-0.49	-0.74	-0.92	0.14	-0.07	-0.59	0.08	-0.12	-0.66	-0.57	-0.05	0.68	44	18	28

Figure 10. Normalized annual anomalies (scorecard) for nutrient inventories and chlorophyll levels during the winter, late spring, and fall surveys. Blue colours indicate anomalies below the mean and reds are anomalies above the mean. Percentages of change in the 2014 values relative to the climatologies are shown to the right of the table.

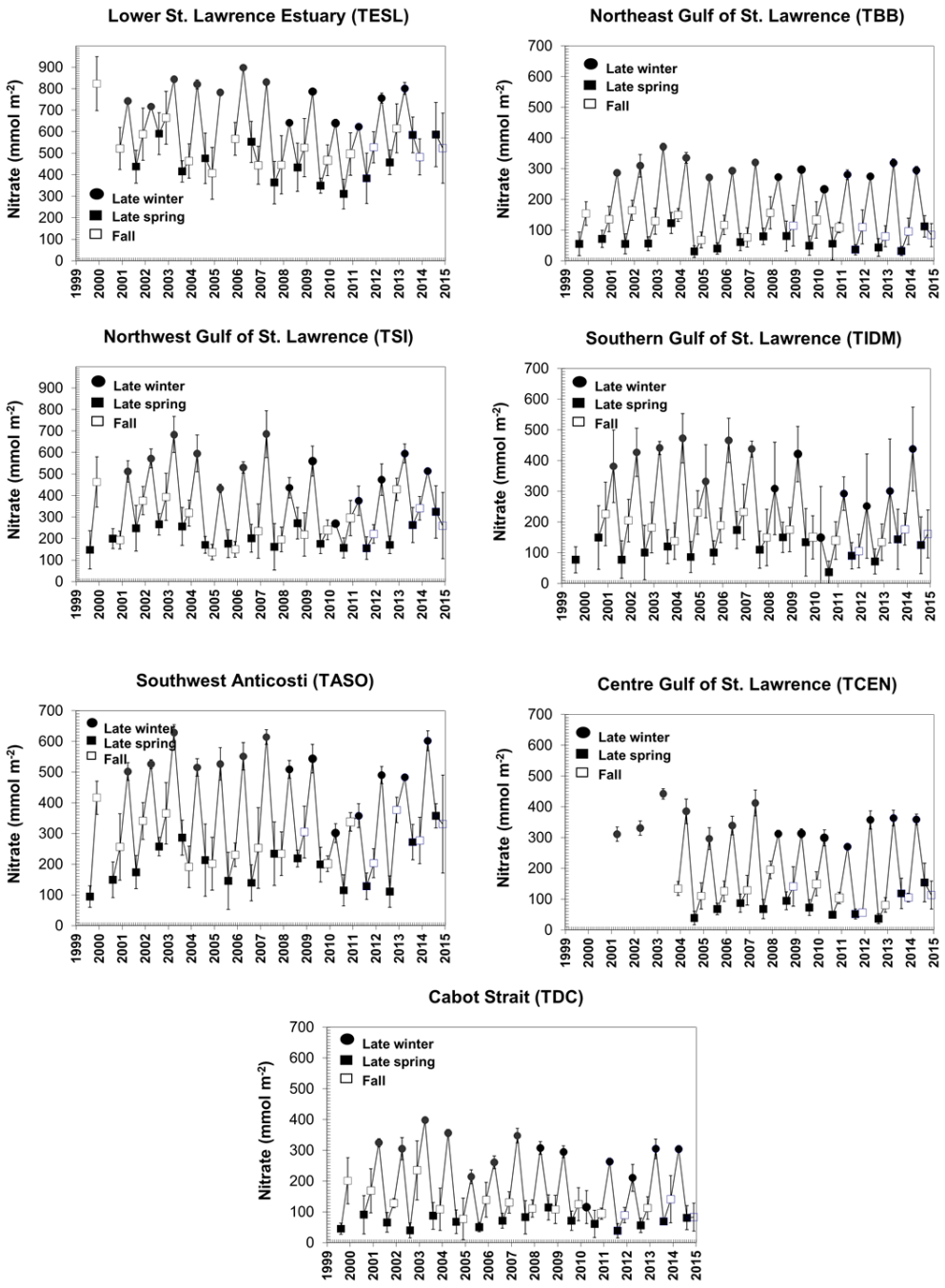

Figure 11. Time series of surface (0–50m) nitrate inventories along the seven AZMP sections from 1999 to 2014. The late winter inventories were calculated using surface (2 m) concentrations × 50 m (assuming that the nitrate concentrations are homogeneous in the winter mixed layer at that time of the year). (Note the different scale for the TESL and TSI graphs.)

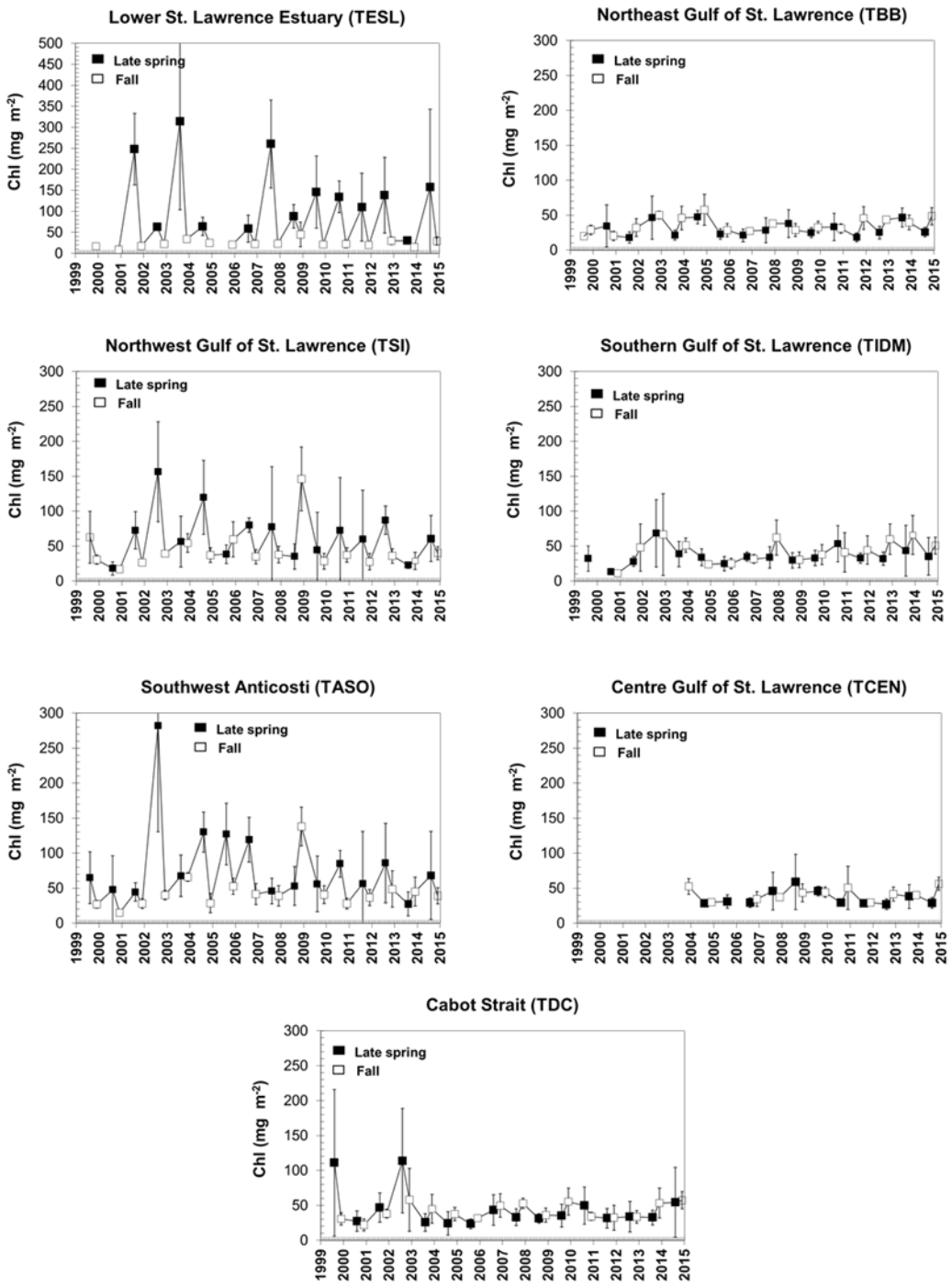

Figure 12. Time series of integrated (0–100 m) chlorophyll biomass along the seven AZMP sections from 1999 to 2014. (Note the different scale for the TESL graph.)

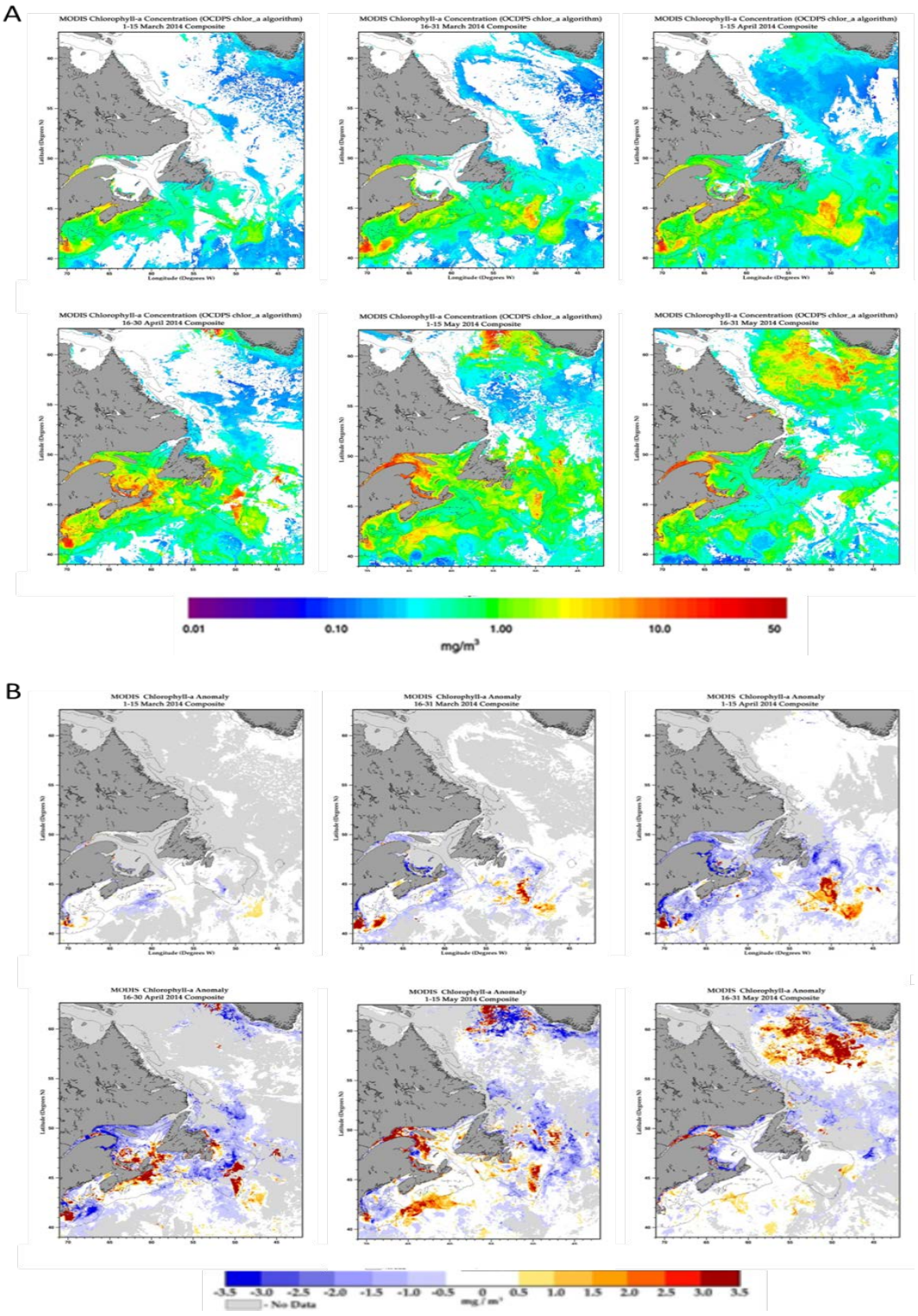

Figure 13. MODIS twice-monthly composite images of surface chlorophyll a (A) and chlorophyll a anomaly (B; based on the 2003–2010 reference period) in the Gulf of St. Lawrence during late winter–early spring 2014 (left to right, top rows: 1–15 March, 16–31 March, 1–15 April; bottom rows: 16–30 April, 1–15 May, 16–31 May).

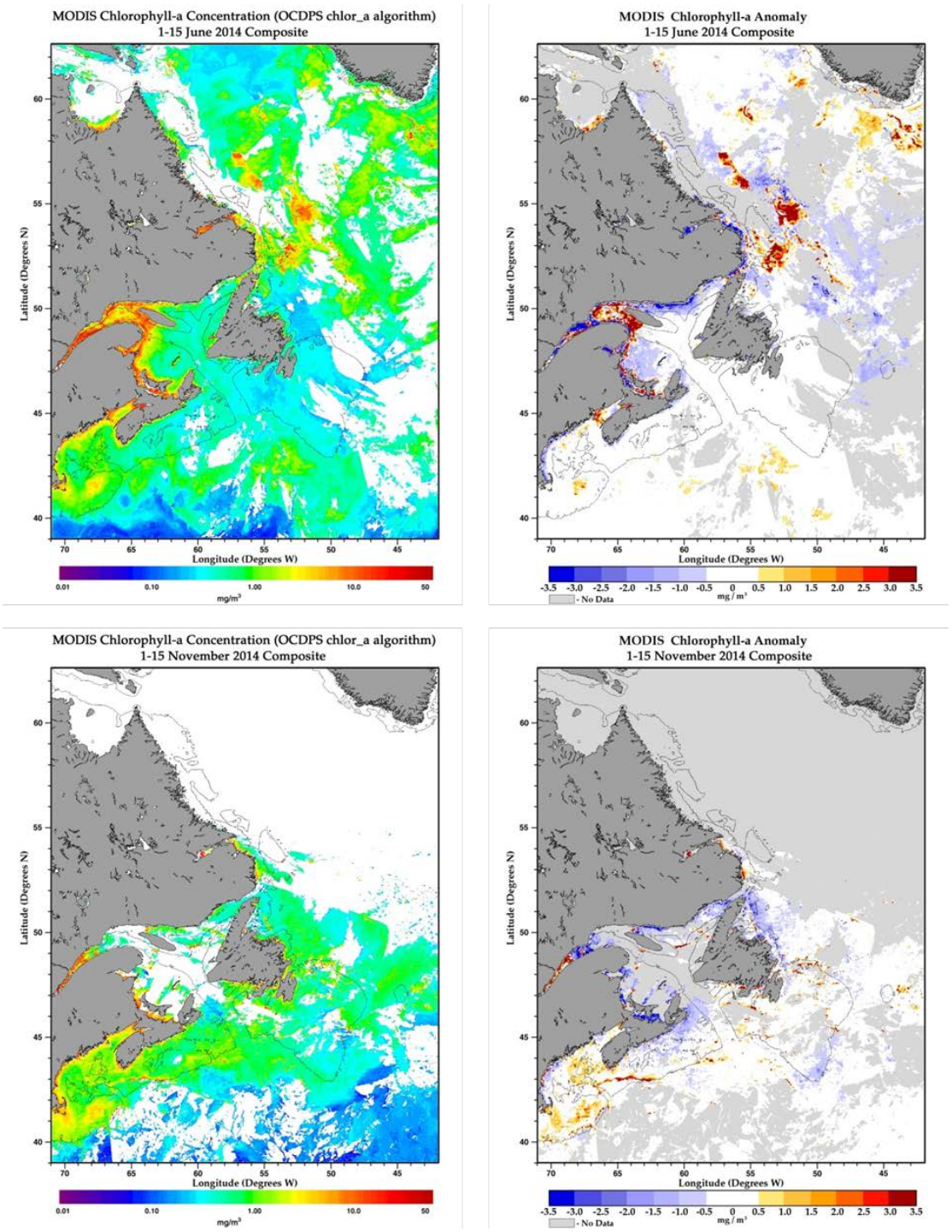

Figure 14. MODIS composite images of surface chlorophyll a (left) and chlorophyll a anomaly (right; based on the 2003–2010 reference period) in the Gulf of St. Lawrence. The images' date intervals (1–15 June and 1–15 Nov. 2013) coincide with those of the late spring (31 May – 11 June 2014) and fall (27 Oct. – 11 Nov. 2014) surveys.

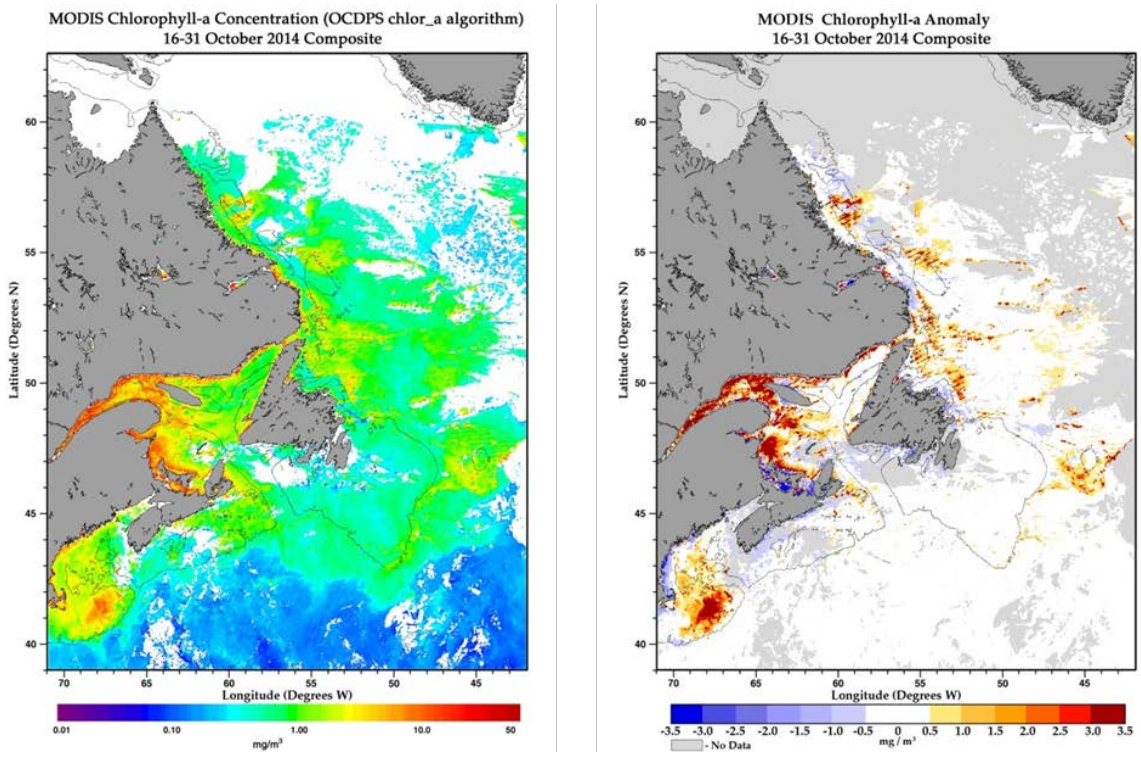

Figure 15. MODIS composite image of surface chlorophyll a (left) and chlorophyll a anomaly (right; based on the 2003–2010 reference period) in the Gulf of St. Lawrence showing the strong positive anomaly in late October 2014 in the Northwestern and Southern Gulf (no concomitant field campaign).

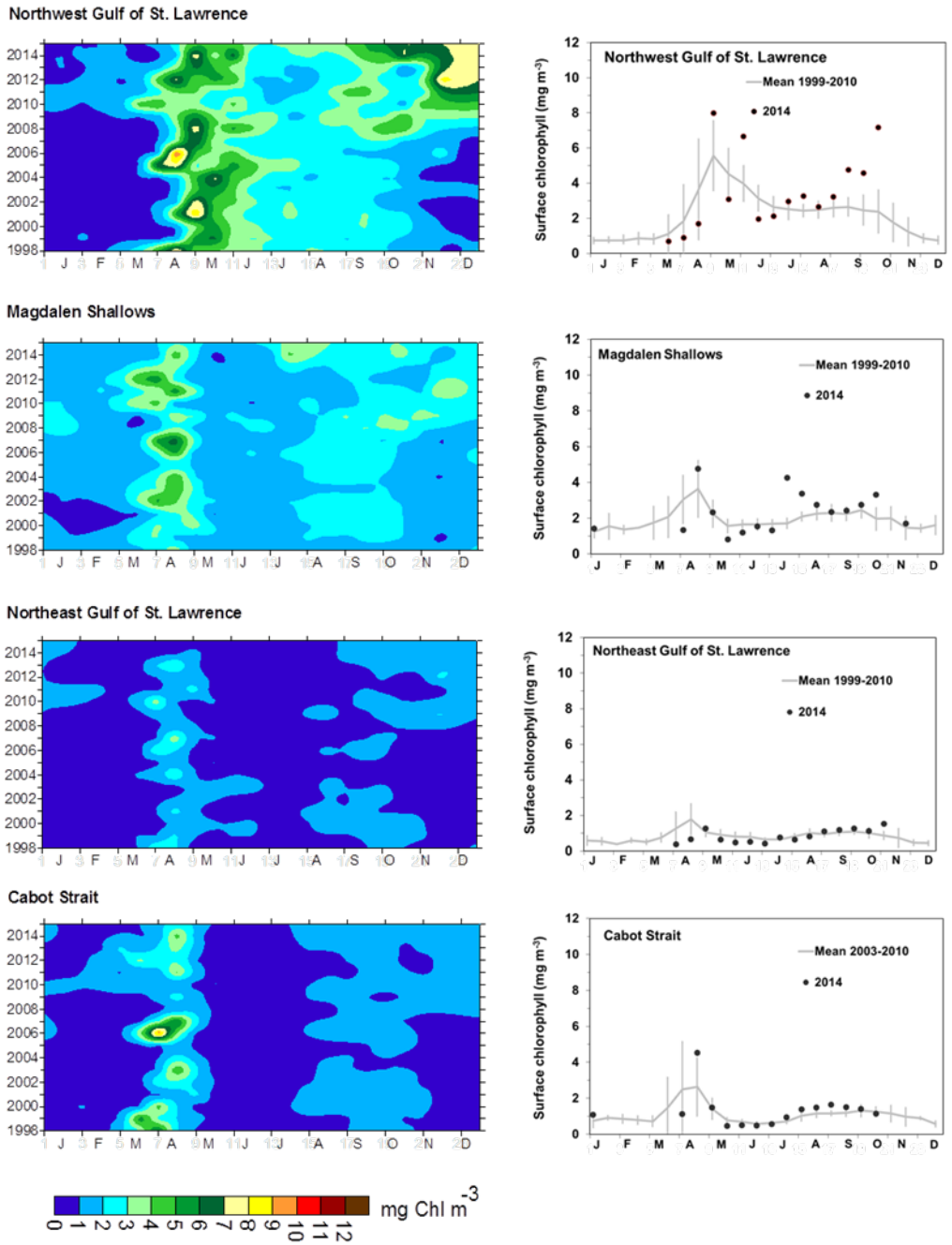

Figure 16. Left panels: Time series of surface chlorophyll a concentrations from twice-monthly SeaWiFS (1998–2007) and MODIS (2008–2015) ocean colour data in the Northwest Gulf of St. Lawrence, Magdalen Shallows, Northeast Gulf of St. Lawrence, and Cabot Strait statistical subregions (see Fig. 3). Right panels: comparison of 2014 (black circles) surface chlorophyll estimates using satellite ocean colour with mean conditions from 1999–2010 (solid line) for the same statistical subregions.

Indices of change in productivity based on SeaWiFS (1998-2007) and MODIS (2008-2014)

Index	Subregion	1998	1999	2000	2001	2002	2003	2004	2005	2006	2007	2008	2009	2010	2011	2012	2013	2014	Mean	S.D.
Annual mean surface Chl	Northeast GSL	0.22	0.74	1.12	0.08	-0.75	0.24	0.16	-1.92	0.07	-0.29	-1.57	0.87	1.26	-0.85	-0.81	1.37	-0.95	0.95	0.10
March to December	Northwest GSL	0.82	-0.63	-0.75	0.05	-0.96	-0.92	-0.70	1.33	0.01	-0.91	1.98	1.00	0.50	0.01	1.60	-0.1	2.10	2.75	0.40
(mg m^{-3})	Magdalen Shallows	-2.46	-1.28	0.37	-1.61	1.75	-0.98	-0.10	-1.74	0.60	0.88	0.30	1.31	-0.28	1.37	-0.57	-0.3	1.64	2.13	0.17
	Cabot Strait	0.71	0.46	0.57	-0.60	0.26	0.05	-0.97	-1.41	2.49	0.35	-0.86	-0.20	-0.14	-0.28	0.01	0.41	0.44	1.19	0.31
Mean surface Chl -	Northeast GSL	1.36	-0.06	-0.92	0.04	-0.39	-0.81	1.69	-1.34	0.48	0.92	-0.61	-0.67	1.66	0.32	-0.58	1.27	-1.79		
March to May	Northwest GSL	2.45	-0.26	-1.66	0.86	-0.62	-1.31	0.08	2.05	0.74	-0.62	0.27	0.25	0.22	-0.85	1.32	0.14	-0.37	3.10	0.63
(mg m^{-3})	Magdalen Shallows	-0.75	-0.52	-0.21	-1.04	0.87	0.64	0.70	-1.39	-0.01	1.62	-1.16	-0.44	0.04	0.55	0.98	-0.4	-0.35	2.53	0.63
	Cabot Strait	1.20	0.86	-0.01	-0.78	-0.03	0.85	-0.71	-1.13	2.20	0.78	-1.12	-0.35	-0.56	-0.01	0.51	0.25	0.37	1.63	0.75
Mean surface Chl -	Northeast GSL	-0.95	0.67	1.61	0.33	-0.38	1.92	0.33	-0.35	-0.34	-1.06	-1.46	0.32	-0.65	-0.93	-1.54	-0.1	-1.19	0.78	0.15
June to August	Northwest GSL	0.50	-0.55	0.09	-0.61	0.36	-0.51	-0.18	2.18	-0.07	-1.55	1.55	-0.19	-0.51	-1.64	-1.12	-1.2	1.10	2.87	0.36
(mg m^{-3})	Magdalen Shallows	-1.16	-0.01	0.38	-0.48	0.55	-1.24	0.39	0.12	1.78	-0.55	0.55	0.16	-1.22	-1.10	-2.32	-0.5	2.56	1.83	0.22
	Cabot Strait	-0.84	-0.78	2.06	0.55	0.54	-0.69	-0.98	-1.68	0.97	-0.07	-0.47	0.18	0.37	-0.85	-1.85	0.13	0.70	0.80	0.13
Mean surface Chl -	Northeast GSL	-0.02	0.72	1.54	-0.08	-0.37	-0.38	-1.50	-1.42	-0.19	-0.67	-0.27	1.85	0.77	-1.02	0.57	0.96	1.55	0.97	0.18
September to December	Northwest GSL	-0.70	-0.60	0.09	-0.41	-1.07	-0.17	-0.98	-0.46	-0.61	-0.24	2.23	1.46	0.76	1.59	1.86	0.17	3.42	2.32	0.76
(mg m^{-3})	Magdalen Shallows	-1.30	-0.80	0.38	-0.34	0.25	-0.95	-0.81	-0.40	-0.26	-0.67	1.35	1.72	0.03	1.10	-0.63	0.32	0.83	2.12	0.48
	Cabot Strait	-0.37	-0.70	1.15	-0.40	0.77	-1.03	-1.23	-0.56	1.64	-1.31	0.56	0.21	0.90	-0.42	-0.76	0.64	0.98	1.20	0.22

Indices of change in spring bloom properties based on SeaWiFS (1998-2007) and MODIS (2008-2014)

Index	Subregion	1998	1999	2000	2001	2002	2003	2004	2005	2006	2007	2008	2009	2010	2011	2012	2013	2014	Mean	S.D.
Start of spring bloom	Northeast GSL	-0.70	-0.03	2.08	0.02	0.24	1.01	-1.10	0.35	-1.11	0.55	0.21	-0.74	-1.47	1.88	-0.35	-0.51	2.37	99	9
(day of the year)	Northwest GSL	-0.74	0.59	0.21	-0.46	1.39	0.10	0.76	-0.87	-0.42	0.32	0.53	0.36	-2.53	-0.74	-0.82	-0.09	0.76	107	13
	Magdalen Shallows	0.37	-0.86	-0.48	0.67	-0.41	0.36	0.99		1.27	-0.25	-6.86	0.73	-2.02	0.43	-1.02	-1.02	1.29	90	13
	Cabot Strait	-0.64	-0.83	-0.19	0.60	0.21	0.78	0.63	0.04	-0.54	0.12	1.67	-0.09	-2.40	0.54		0.10	0.78	92	14
Spring bloom duration	Northeast GSL	-0.39	-0.37	-0.79	-0.28	0.51	2.90	0.23	-0.82	-0.06	-0.53	0.12	-0.32	-0.60	-0.99	0.02	-0.25	-0.84	35	22
(days)	Northwest GSL	-0.12	0.48	2.08	0.43	-1.24	1.35	0.46	-0.85	-0.74	-0.01	-0.60	-0.95	-0.41	0.16	-0.68	0.93	-0.79	42	22
	Magdalen Shallows	-0.11	-0.49	1.91	-0.71	0.23	0.05	-1.32	-2.23	-1.24	0.72	-2.23	-0.02	0.86	-0.13	-0.22	0.94	-1.10	37	16
	Cabot Strait	0.09	-0.55	-1.23	0.93	-1.24	-1.34	0.13	0.54	0.28	0.57	-0.70	0.88	1.74	-0.49		0.17	-1.29	30	12
Spring bloom magnitude	Northeast GSL	1.79	-0.56	-1.23	0.29	-0.30	1.37	0.71	-1.43	0.75	1.17	-0.70	-1.08	1.00	-0.98	-0.37	0.82	-1.59	39	18
(mg Chl m^{-2})	Northwest GSL	0.80	0.22	1.34	0.69	-1.49	1.13	1.35	-0.73	-0.27	0.45	-0.61	-0.91	-1.16	-1.11	0.57	0.78	-0.68	156	51
	Magdalen Shallows	-0.10	-0.91	-0.26	-0.66	0.59	0.75	-1.05	-1.64	-0.87	1.99	-1.64	-0.45	0.87	0.61	1.48	-0.56	-0.29	81	49
	Cabot Strait	2.57	0.41	-0.37	-0.34	0.06	-0.18	-0.45	-0.98	2.42	1.31	-1.24	-0.11	-0.52	-0.03		-0.30	-0.11	67	42
Spring bloom amplitude	Northeast GSL	2.55	-0.19	-0.35	0.60	-0.79	-0.95	0.17	-0.63	0.61	2.34	-0.83	-0.82	2.43	0.78	-0.47	1.07	-0.90	1.68	0.82
(mg Chl m^{-3})	Northwest GSL	0.82	-0.90	-1.50	-0.39	1.23	-1.10	0.19	0.91	1.37	0.14	0.18	1.01	-1.13	-1.84	2.60	-0.94	0.78	5.94	1.50
	Magdalen Shallows	-0.03	-1.15	-1.45	-0.33	0.61	1.13	-0.32	-2.64	0.17	1.77	-2.64	-0.70	0.27	1.20	2.94	-1.42	1.67	3.16	1.20
	Cabot Strait	1.93	0.65	0.46	-0.79	1.24	1.00	-0.64	-1.15	1.57	0.48	-1.16	-0.63	-1.03	0.10		-0.53	1.02	3.65	2.32

Figure 17. Annual anomalies (scorecard) of productivity indices (chlorophyll means for various time periods) and indices of change of spring bloom properties across Gulf of St. Lawrence statistical subregions from 1998 to 2014. The reference period used to compute annual anomalies was 1999–2010. Blue colours indicate anomalies below the mean and reds are anomalies above the mean. The climatological means and standard deviations are shown to the right of the table.

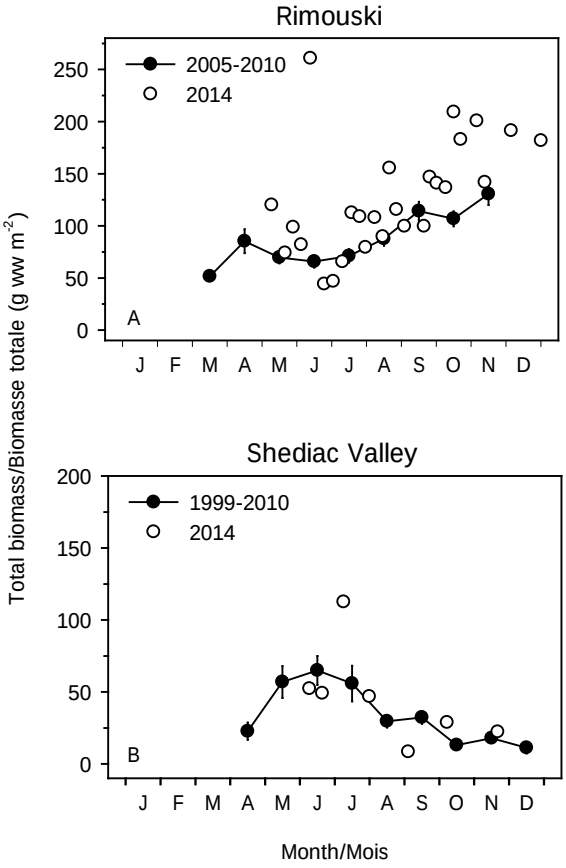

Figure 18. Comparison of total zooplankton biomass in 2014 (white circles) with the monthly climatology from Rimouski (2005–2010) and Shediac Valley (1999–2010) stations (solid lines). Vertical lines are standard errors of the annual averages.

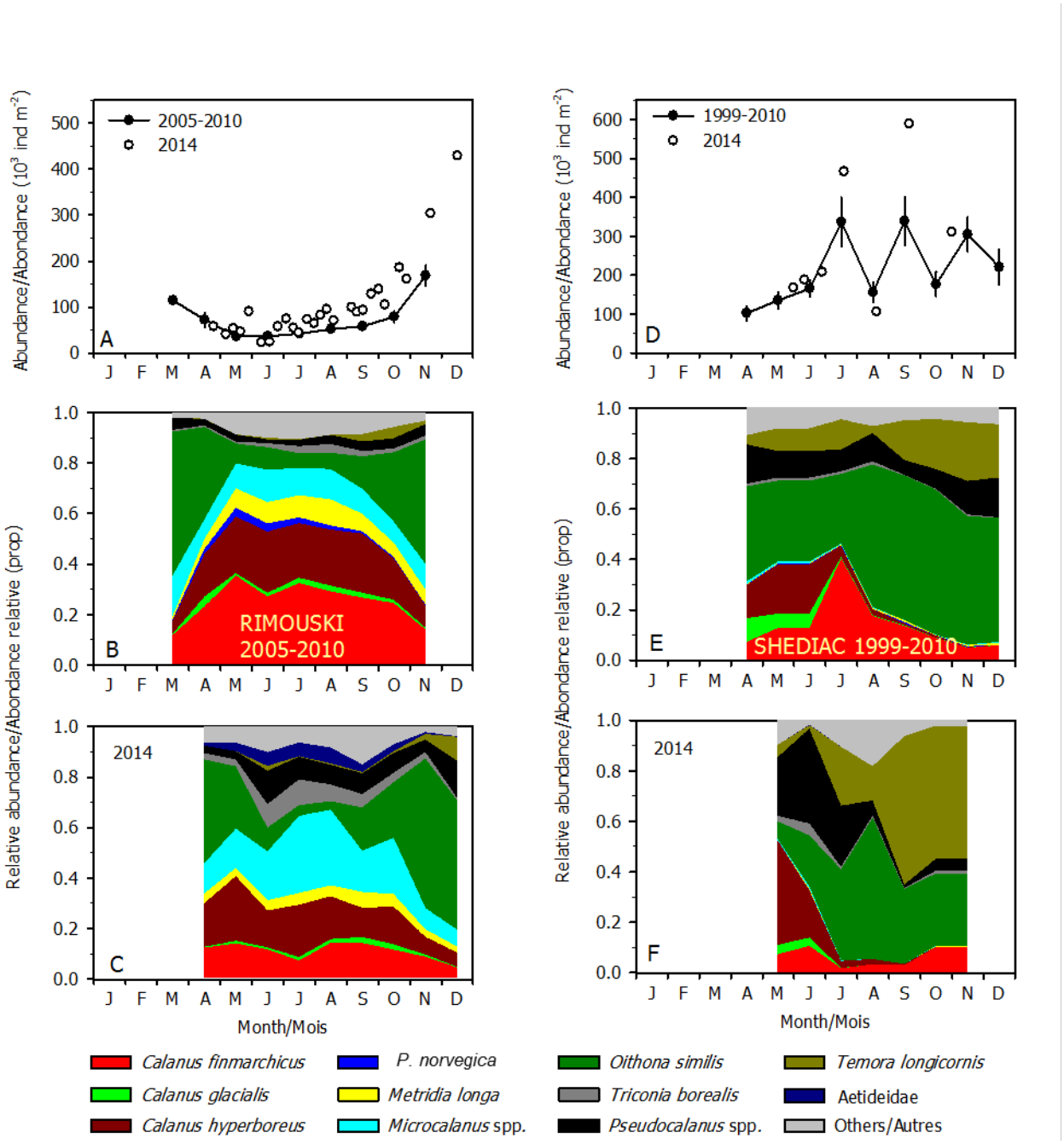

Figure 19. Seasonal variability in abundances of the 10 dominant copepod species at Rimouski (left panels) and Shediac Valley (right panels) stations. Climatologies of combined counts for the reference periods (solid lines with standard errors) are plotted with data from 2014 (white circles)(including the "others" category; A, D). Seasonal variability by species for the reference periods (B, E) and for 2014 (C, F) are also shown. In 2014, the Aetideidae group displaced Paraeuchaeta norvegica at Rimouski station (C).

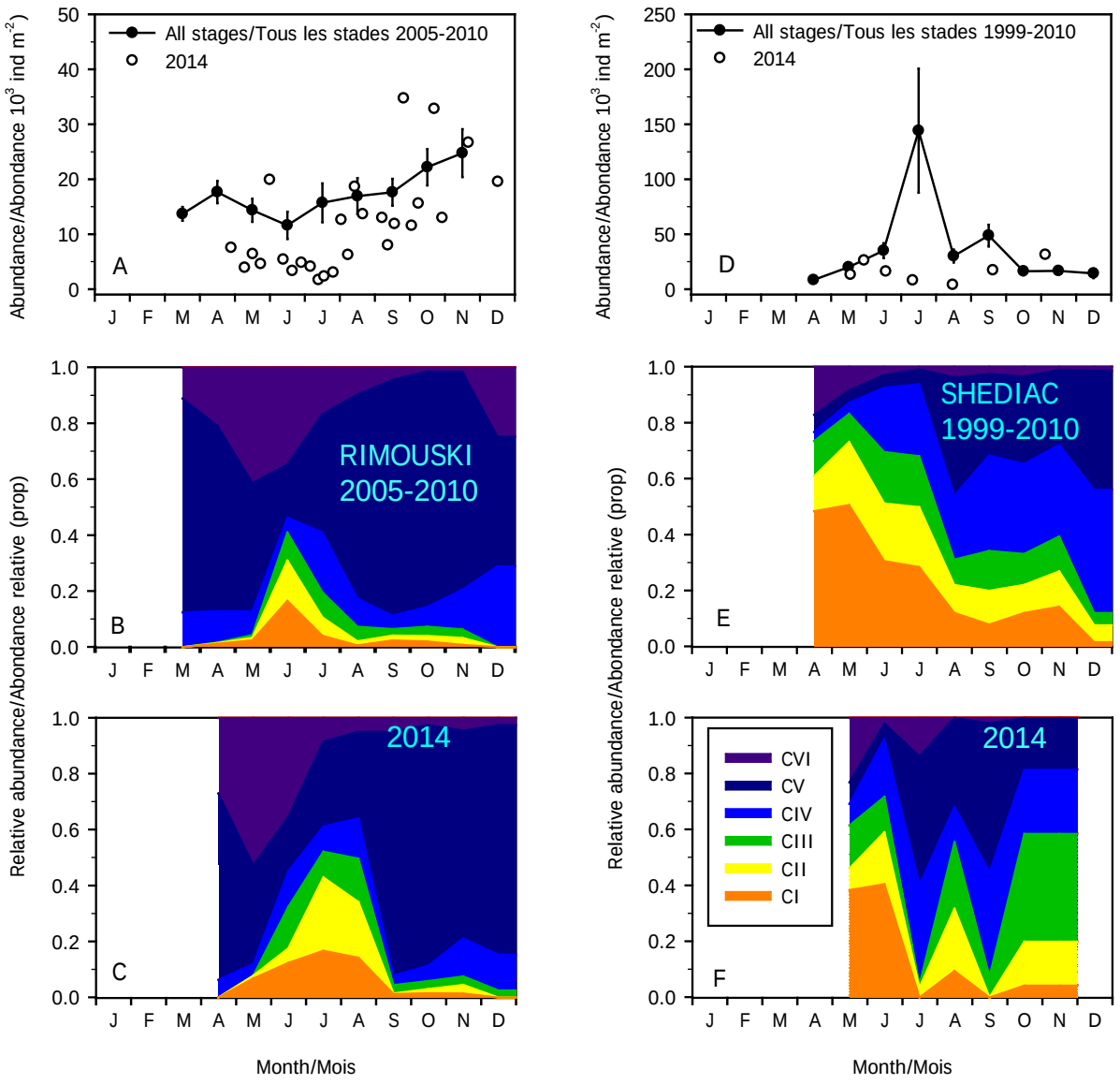

Figure 20. Seasonal variability in Calanus finmarchicus copepodite abundances at Rimouski (left panels) and Shediac Valley (right panels) stations. Climatologies of combined counts for the reference periods (solid lines with standard errors) are plotted with data from 2014 (white circles) (A, D). Seasonal variabilities for the individual copepodite stages for the reference periods (B, E) and for 2014 (C, F) are also shown.

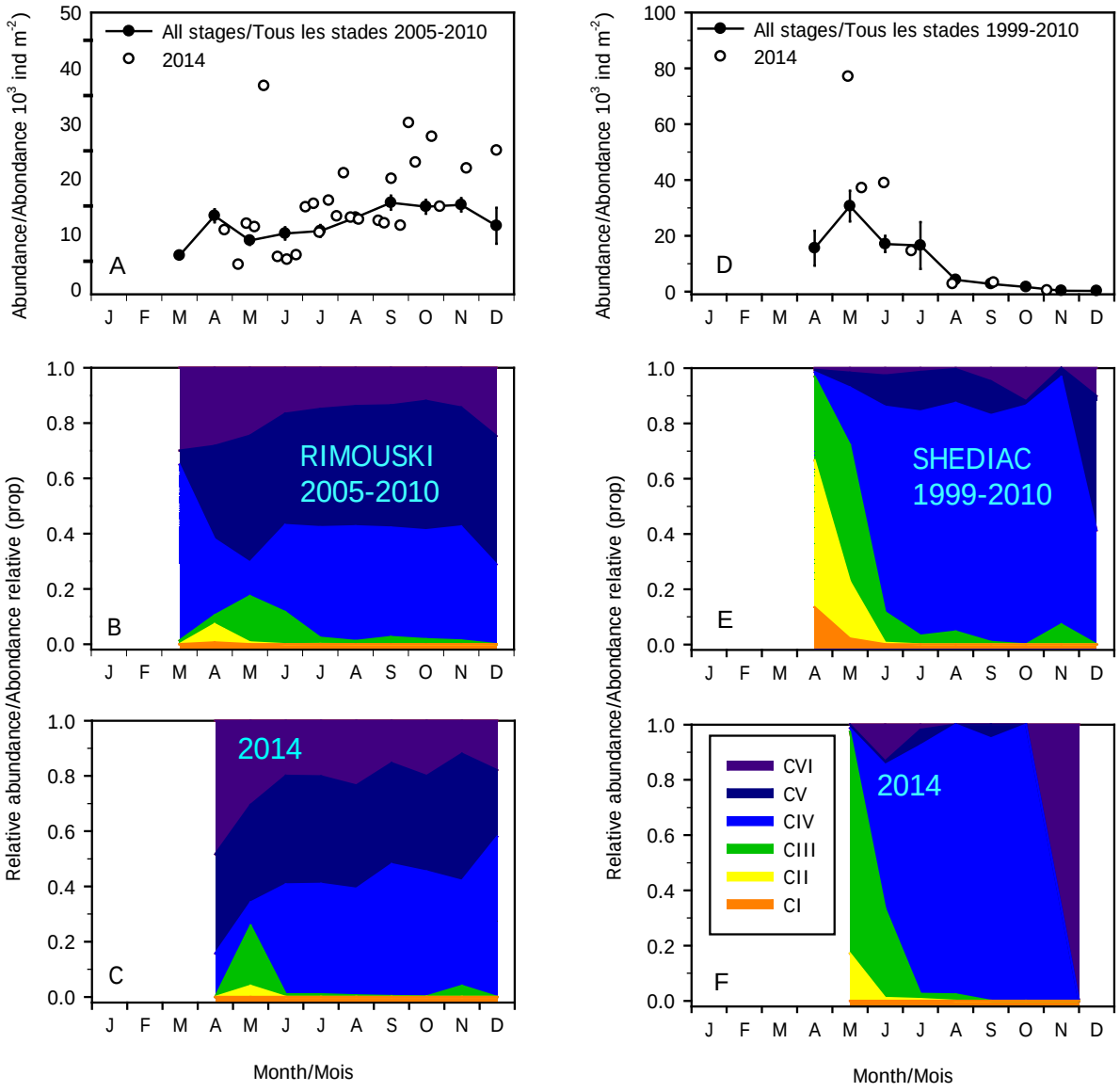

Figure 21. Seasonal variability in Calanus hyperboreus copepodite abundances for Rimouski (left panels) and Shediac Valley (right panels) stations. Climatologies of combined counts for the reference periods (solid lines with standard errors) are plotted with data from 2014 (white circles) (A, D). Seasonal variability for the individual copepodite stages for the reference periods (B, E) and for 2014 (C, F) are also shown.

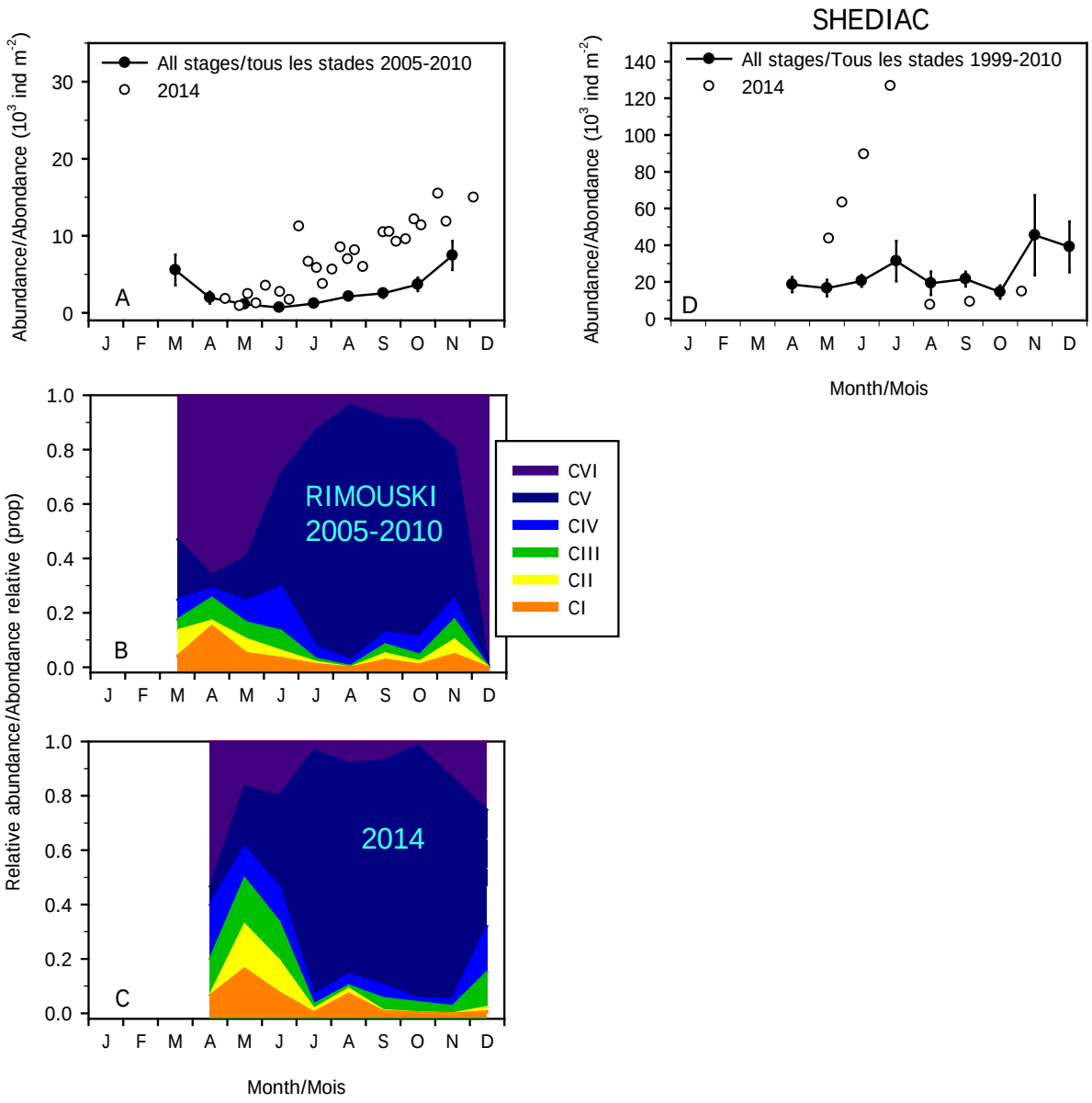

Figure 22. Seasonal variability in Pseudocalanus spp. copepodite stage abundances for Rimouski (left panels) and Shediac Valley (right panel) stations. Climatologies of combined counts for the reference periods (solid lines with standard errors) are plotted with data from 2014 (white circles) (A, D). Seasonal variability for the individual copepodite stages for the reference periods (B) and for 2014 (C) are also shown. No stage information is available for Shediac Valley.

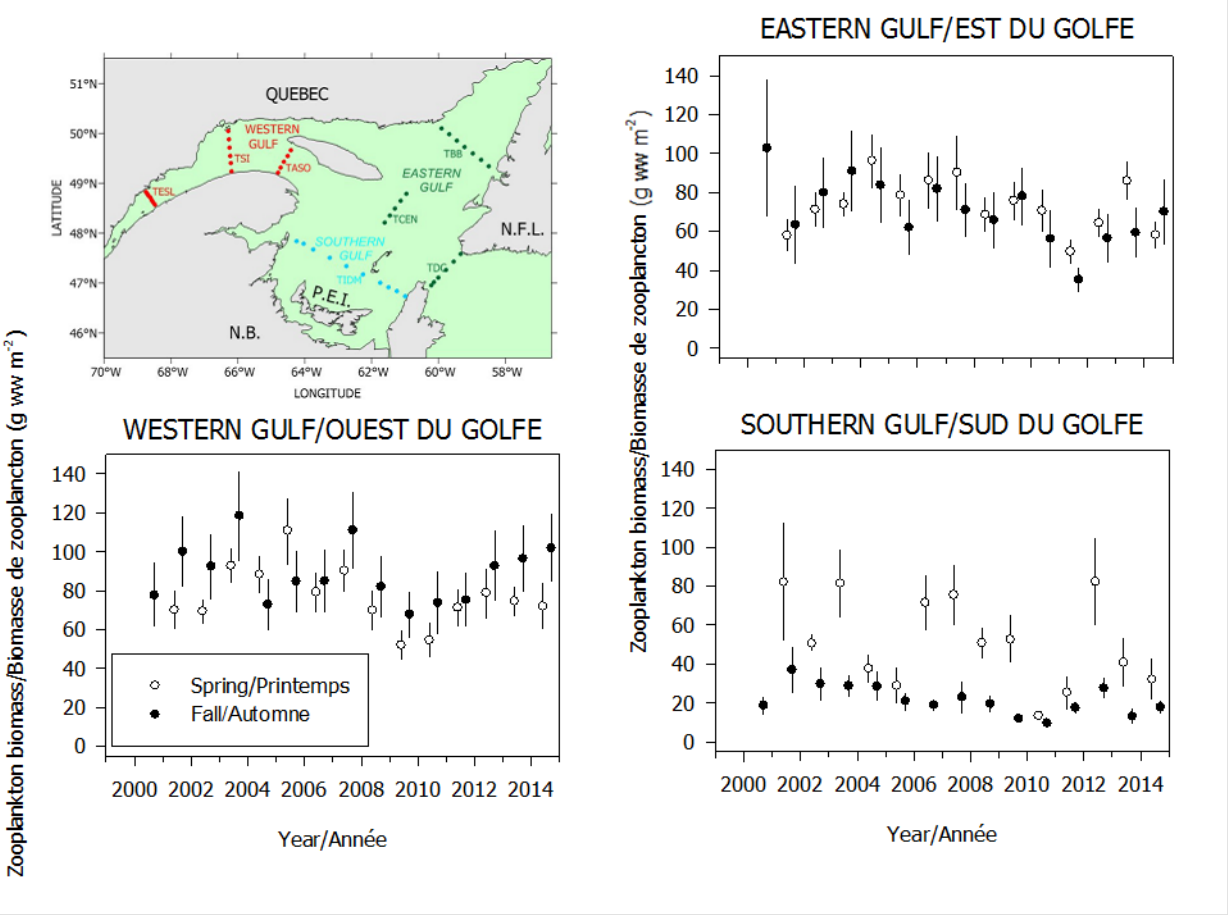

Figure 23. Mean total zooplankton biomass during spring and fall for three subregions of the Estuary and Gulf of St. Lawrence from 2000 to 2014. Vertical lines represent standard errors.

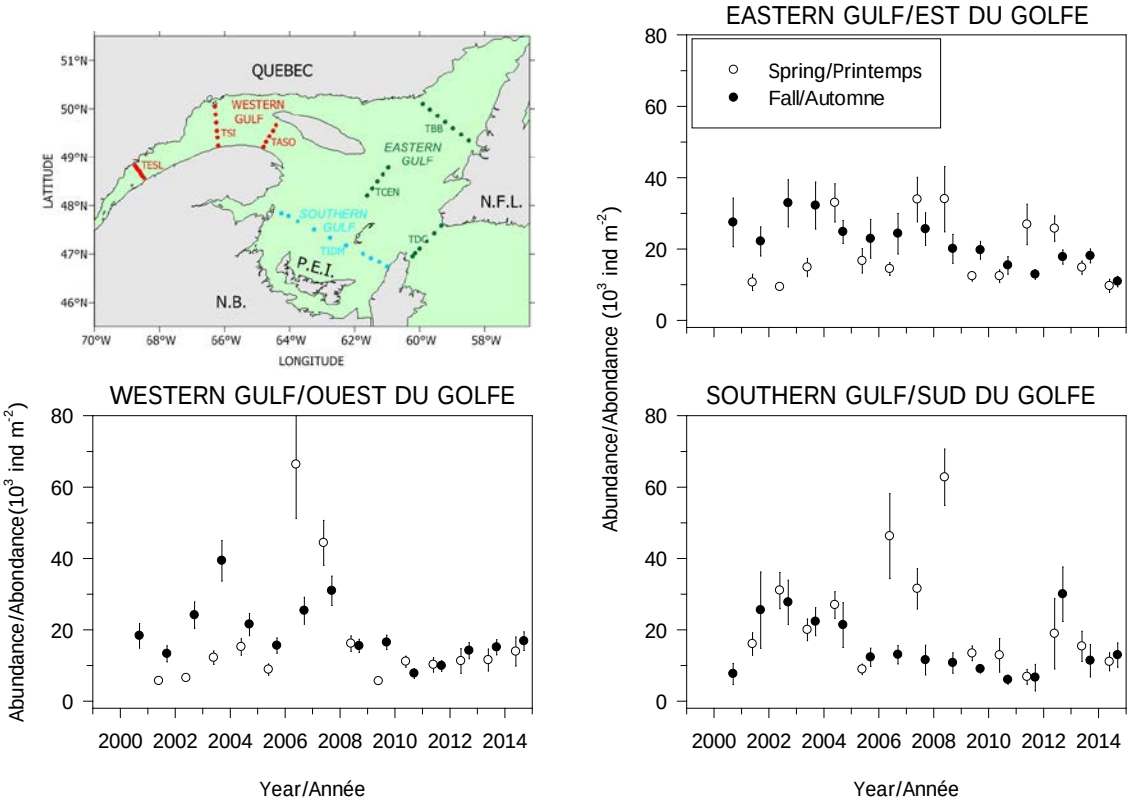

Figure 24. Mean total abundance of Calanus finmarchicus during spring and fall for three subregions of the Estuary and Gulf of St. Lawrence from 2000 to 2014. Vertical lines represent standard errors.

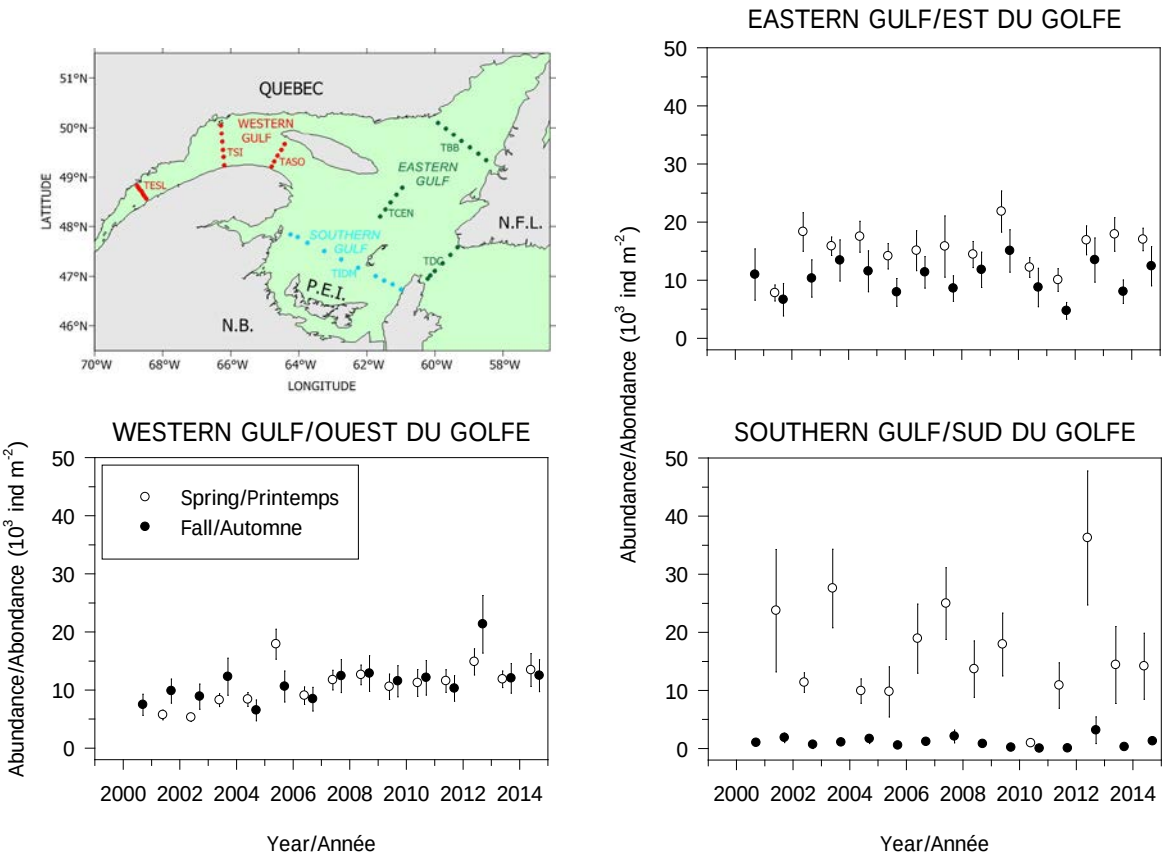

Figure 25. Mean total abundance of Calanus hyperboreus during spring and fall for three subregions of the Estuary and Gulf of St. Lawrence from 2000 to 2014. Vertical lines represent standard errors.

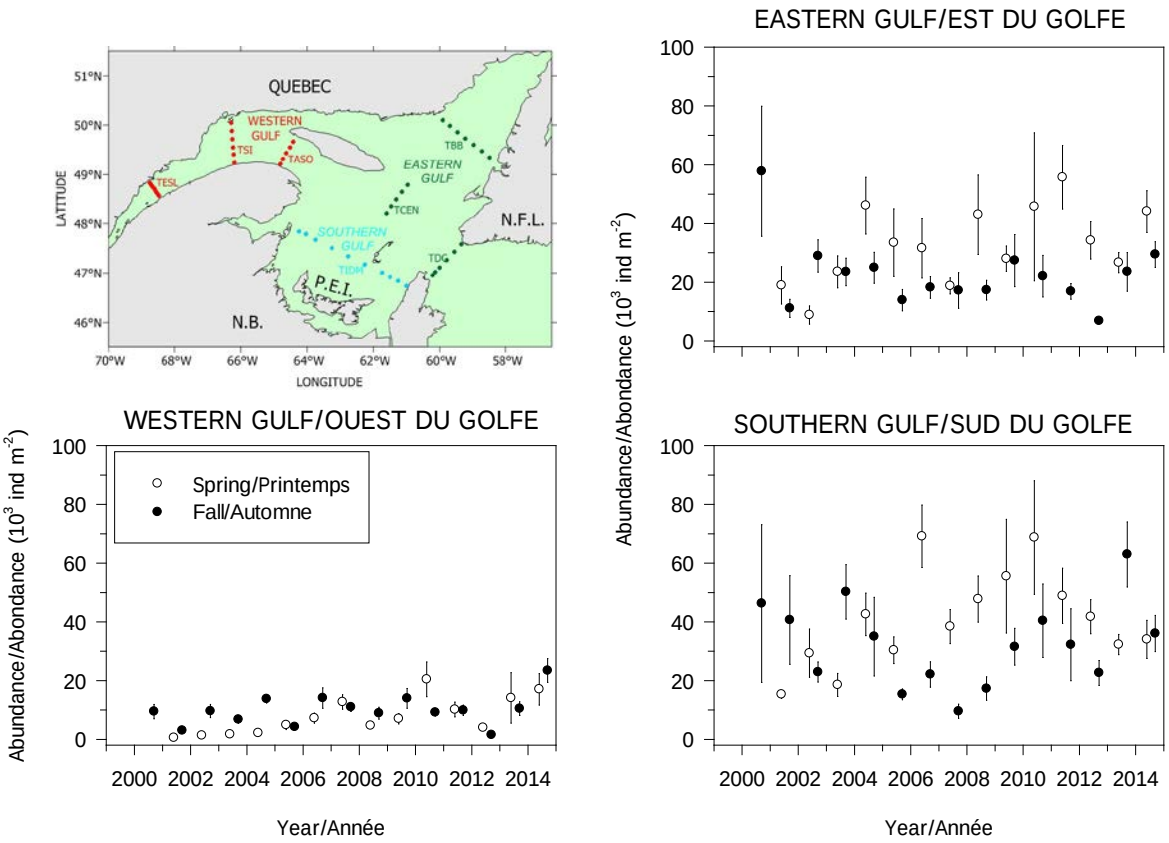

Figure 26. Mean total abundance of <u>Pseudocalanus</u> spp. during spring and fall for three subregions of the Estuary and Gulf of St. Lawrence from 2000 to 2014. Vertical lines represent standard errors.

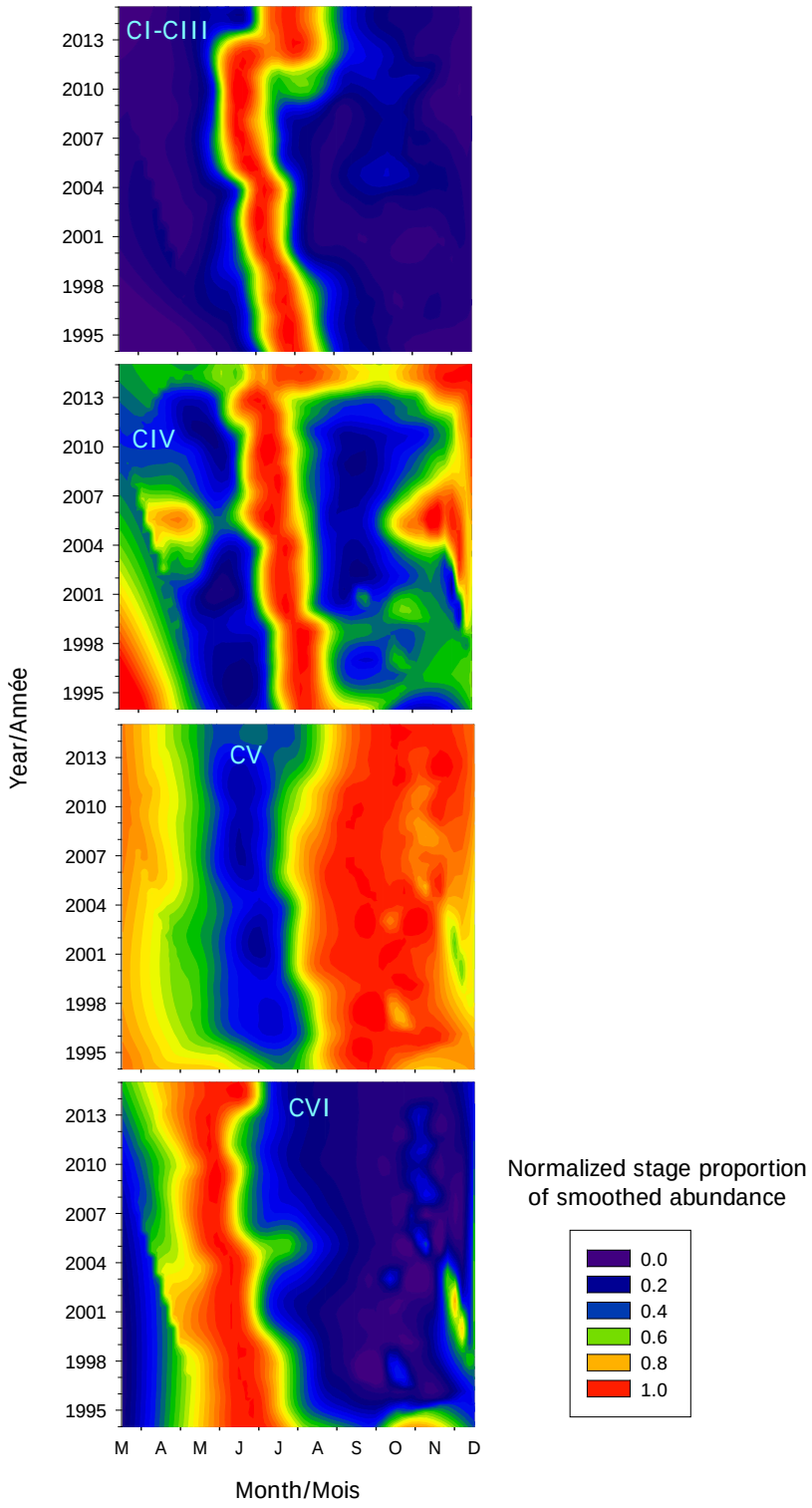

Figure 27. Seasonal cycle in relative stage proportions (percentage of total abundance) of stage CI–III, CIV, CV, CVI (male + female) Calanus finmarchicus copepodites from 1994 to 2014 at Rimouski station.

Group	Region	1999	2000	2001	2002	2003	2004	2005	2006	2007	2008	2009	2010	2011	2012	2013	2014
C. finmarchicus	Rimouski							-0.94	-0.03	1.78	0.30	-0.19	-0.91	-0.76	-0.58	-0.98	-0.43
	Shediac	-0.55	-0.33	-0.25	-0.33	2.59	1.30	-0.49	0.13	-0.42	0.15	-0.87	-0.91	-1.05	-0.33	-1.02	-0.84
	wGSL		-0.15	-0.87	-0.40	0.51	-0.17	-0.58	2.17	1.50	-0.36	-0.76	-0.90	-0.84	-0.61	-0.57	-0.38
	sGSL		-1.35	-0.02	0.97	0.09	0.44	-1.03	0.99	0.13	1.75	-0.97	-1.00	-1.44	0.44	-0.74	-0.89
	eGSL		0.92	-1.06	-0.19	0.39	1.24	-0.44	-0.52	1.34	0.85	-1.08	-1.46	-0.37	-0.08	-1.01	-2.09
Pseudocalanus spp.	Rimouski							-1.22	-0.42	0.68	-0.69	0.10	1.55	1.61	-1.14	-0.41	6.43
	Shediac	1.40	-0.88	2.01	-0.16	0.00	-0.63	0.44	-1.55	-0.93	-0.31	0.14	0.46	1.03	-0.17	-0.41	3.00
	wGSL		0.39	-1.59	-0.64	-0.95	-0.14	-0.91	0.69	1.01	-0.30	0.66	1.77	0.53	-1.37	1.12	3.26
	sGSL		0.83	-0.88	-0.86	-0.18	0.23	-1.16	0.77	-1.06	-0.34	0.60	2.05	0.34	-0.36	0.94	-0.13
	eGSL		2.50	-1.11	-0.80	-0.40	0.70	-0.36	-0.27	-0.87	0.16	-0.05	0.50	0.73	-0.65	-0.27	0.72
Total copepods	Rimouski							-1.48	-0.68	0.97	-0.20	1.15	0.24	1.36	-0.38	-0.38	3.93
	Shediac	0.71	-0.84	-0.03	-0.64	0.76	-0.51	-0.19	-0.76	0.23	2.63	-0.82	-0.54	-0.28	-0.46	-1.74	1.53
	wGSL		0.08	-1.65	-0.95	-1.15	-0.53	-0.21	1.42	0.42	0.88	0.43	1.25	-0.25	-1.43	-1.21	1.37
	sGSL		-0.66	-0.31	0.46	-0.75	-0.75	-1.79	1.00	-0.19	1.64	1.05	0.29	-0.02	0.21	-1.75	-0.03
	eGSL		2.07	-1.99	0.07	-0.14	0.74	-0.84	-0.45	-0.02	0.37	-0.13	0.32	0.53	-0.67	-1.01	0.01
Non copepods	Rimouski							-0.95	-0.72	1.29	-0.96	0.47	0.88	1.88	-1.13	2.49	20.07
	Shediac	1.94	-1.17	0.65	-0.14	-1.15	-0.79	0.78	0.40	0.21	1.00	-1.17	-0.56	0.19	4.35	0.31	8.09
	wGSL		-0.63	-0.86	-0.81	-0.30	-0.74	-0.60	1.42	2.19	0.59	-0.14	-0.13	1.24	-0.26	-0.37	1.06
	sGSL		-0.67	-0.91	-0.27	-0.66	-0.76	0.52	-0.16	0.11	-0.06	0.17	2.70	1.94	1.73	2.38	3.42
	eGSL		-0.58	-1.44	-0.69	-1.14	0.26	1.68	1.25	1.10	-0.07	0.03	-0.42	4.37	-0.34	1.73	3.70

Figure 28. Normalized annual anomalies (scorecard) for four zooplankton categories at the high-frequency monitoring sites and the three subregions of the Estuary and Gulf of St. Lawrence (reference period: 1999–2010 [2005–2010 for Rimouski]). Blue colours indicate anomalies below the mean and reds are anomalies above the mean.

	Region	1999	2000	2001	2002	2003	2004	2005	2006	2007	2008	2009	2010	2011	2012	2013	2014
C. hyperboreus	Rimouski							0.83	-0.12	0.18	1.34	-1.21	-1.01	0.65	0.91	0.71	1.11
	Shediac	0.16	0.76	-0.52	-1.32	1.15	-0.74	1.81	1.14	-0.15	-1.10	-0.73	-0.45	-1.13	2.24	-0.43	1.17
	wGSL		-1.09	-0.91	-1.26	0.15	-1.06	1.43	-0.54	0.90	1.19	0.46	0.73	0.40	3.54	0.84	1.26
	sGSL		-1.26	-1.08	-0.12	1.60	-0.13	-0.36	0.69	1.43	0.08	0.47	-1.33	-0.30	2.76	0.10	0.25
	eGSL		-0.95	-0.73	0.50	0.58	0.71	-0.89	0.05	-0.38	-0.03	2.29	-1.15	-2.47	0.87	-0.09	0.67
Small calanoids	Rimouski							-1.19	-0.69	-0.04	-0.48	1.21	1.18	3.69	1.25	0.90	4.33
	Shediac	0.54	-0.77	0.05	-0.48	-0.25	-0.84	-0.61	-0.99	0.20	2.76	0.05	0.34	1.54	-0.45	-0.49	2.77
	wGSL		0.05	-1.31	-0.94	-1.10	-0.43	-0.96	1.18	0.39	1.39	0.60	1.12	0.98	-0.45	0.00	3.86
	sGSL		-0.04	-1.46	-0.39	0.25	-0.43	-0.97	1.10	-1.30	0.88	1.42	0.93	2.50	0.22	-0.04	0.65
	eGSL		2.20	-1.53	-0.24	0.46	1.03	-0.54	-0.38	-0.94	-0.07	-0.28	0.28	1.38	-0.48	-0.44	0.51
Large calanoids	Rimouski							-0.12	-0.10	1.65	0.51	-0.79	-1.16	-0.21	-0.35	-0.66	0.07
	Shediac	-0.33	0.07	-0.35	-0.87	2.57	0.84	0.40	0.42	-0.48	-0.25	-1.09	-0.95	-1.42	0.74	-1.18	-0.16
	wGSL		-0.16	-1.01	-0.55	0.35	-0.39	0.00	2.00	1.71	-0.31	-0.89	-0.76	-0.81	-0.06	-0.60	-0.32
	sGSL		-1.64	0.67	0.50	0.49	0.13	-1.01	0.92	0.58	1.34	-0.57	-1.41	-1.40	1.43	-0.67	-0.63
	eGSL		0.63	-1.79	-0.36	0.27	1.06	-0.52	-0.34	1.56	0.63	0.19	-1.34	-0.99	0.74	-0.69	-1.01
Cyclopoids	Rimouski							-1.15	-0.39	-0.37	-0.46	1.60	0.77	-0.39	-1.10	-0.42	2.19
	Shediac	1.28	-0.75	0.05	0.02	-0.03	-0.69	0.01	-0.71	0.70	2.25	-1.08	-1.05	-1.54	-1.04	-2.29	-0.38
	wGSL		0.17	-1.53	-0.82	-1.26	-0.44	0.07	0.78	-0.34	0.84	0.77	1.77	-0.45	-2.00	-1.59	0.54
	sGSL		0.00	-1.74	1.01	-1.21	-0.48	-1.07	0.29	0.86	1.29	0.72	0.33	-1.41	-0.31	-1.97	-0.12
	eGSL		1.93	-1.78	0.42	-0.65	0.35	-1.11	-0.50	0.24	0.53	-0.17	0.72	0.17	-1.28	-1.39	-0.24
Copepod: warm species	Rimouski							-1.00	-0.83	1.55	-0.21	-0.36	0.85	7.82	0.26	6.54	9.67
	Shediac	1.94	0.23	1.78	-0.14	0.09	-0.85	-0.63	-1.23	-0.79	0.53	-0.51	-0.42	-1.42	0.83	-1.38	1.13
	wGSL		0.62	-0.84	-1.04	-1.01	-0.91	-0.73	-0.42	0.84	1.74	0.82	0.93	2.51	0.62	4.11	14.52
	sGSL		-0.01	-0.70	-0.21	-0.52	-0.68	-0.61	-0.16	-0.55	-0.11	2.70	0.85	1.09	7.11	-0.26	0.04
	eGSL		2.40	-0.97	-0.74	-0.83	-0.77	0.30	0.30	-0.56	0.31	0.88	-0.33	2.98	3.76	0.29	2.02
Copepod: cold species	Rimouski							1.67	-0.12	-0.02	-1.29	-0.63	0.39	0.30	-0.87	-1.07	0.00
	Shediac	0.11	1.66	-0.08	-1.45	-1.07	-0.36	1.98	-0.42	-0.61	0.27	-0.39	0.35	-1.00	3.25	-1.16	0.43
	wGSL		-0.81	0.20	1.03	-0.88	0.19	2.09	-0.44	0.42	-1.03	-1.20	0.43	-0.58	-0.76	-1.62	-0.86
	sGSL		-1.24	1.89	-1.10	-0.96	-0.52	0.32	-0.12	0.36	0.52	1.33	-0.47	-0.48	0.80	-0.65	0.56
	eGSL		-0.76	0.31	-1.04	-0.54	-0.69	-0.04	-0.76	2.35	-0.40	0.68	0.88	0.21	1.22	-0.25	0.42

Figure 29. Normalized annual anomalies (scorecard) for six categories of zooplankton assemblages at the high-frequency monitoring sites and the three subregions of the Estuary and Gulf of St. Lawrence (reference period: 1999–2010 [2005–2010 for Rimouski station]). Blue colours indicate anomalies below the mean and reds are anomalies above the mean. Small calanoids: mostly neritic species such as Pseudocalanus spp., Acartia spp., Temora longicornis, and Centropages spp.; large calanoids: mostly Calanus and Metridia species; cyclopoids: mostly Oithona spp. and Triconia spp.; warm-water species: Metridia lucens, Centropages spp., Paracalanus spp., and Clausocalanus spp.; and cold/arctic species: Calanus glacialis and Metridia longa.